QUASI-ELASTIC AND ELASTIC CHARGE-EXCHANGE DIFFERENTIAL CROSS SECTIONS: CRITICAL REVIEW

F. Lehar

SPP DAPNIA, CEA Saclay, Gif-sur-Yvette Cedex, France,
and IEAP CTU, Prague, Czech Republic

QUASI-ELASTIC AND ELASTIC CHARGE-EXCHANGE DIFFERENTIAL CROSS SECTIONS: CRITICAL REVIEW

F. Lehar

SPP DAPNIA, CEA Saclay, Gif-sur-Yvette Cedex, France,
and IEAP CTU, Prague, Czech Republic

The present paper is a critical review checking expressions for $R_{np}(\pi)$ in different amplitude representations, listing numerical values of elastic np quantities and results of existing quasi-elastic experiments. Conclusions and statements of some authors and the validity of the relevant theory are discussed.

Представлен критический обзор, в котором анализируется справедливость выражений для $R_{np}(\pi)$ при различных представлениях амплитуд, приводятся численные значения величин для упругого np-рассеяния и результаты существующих квазиупругих измерений. Обсуждаются утверждения и выводы различных авторов, а также справедливость соответствующих теоретических построений.

PACS: 25.40.Kv

1. INTRODUCTION

In 1950–1951 Chew [1, 2] and Pomeranchuk [3] proposed to measure the charge-exchange reaction $nd \rightarrow (nn) + p$ under defined kinematical conditions, in order to determine the spin-dependent part of the $np \rightarrow np$ elastic differential cross section in the backward direction. To produce the polarized beams at «high» energies (a few hundreds of MeV) in the early 1950s was not easy, and no polarized targets existed. Consequently, a suggestion to use for such a purpose unpolarized neutrons scattered on unpolarized deuteron and proton targets was attractive for physicists. The theory of this proposal was then developed by Watson [4], Schmushkevich [5], Migdal [6], Lapidus [7], Dean [8, 9], etc. Later, the theory was extended for the polarized particles by Arvieux, Boudard, Bugg, Wilkin, et al. (see, e.g., [10]).

The protons and neutrons bound in deuterons are in the $^3S_1$ and $^3D_1$ states, and their spins are parallel. In the nd backward charge-exchange process, the two slow remaining identical particles need to be in spin-singlet states $^1S_0$, $^1D_2$, due to the Pauli principle.

In the first part of the experiment, the quasi-elastic $nd \rightarrow (nn) + p$ differential crosss section is to be determined. The outgoing proton momentum coincides

with the incident neutron one. It needs to be larger than the intrinsic momenta of nucleons in the deuteron. The impulse approximation (IA) has been assumed; i.e., in the final state of the two remaining identical nucleons their interaction can be neglected [11]. This $nd \rightarrow (nn) + p$ reaction is taken here as an example, since $pd \rightarrow (pp) + n$ or $dp \rightarrow (pp) + n$ reactions are equally conceivable.

In the second part is determined the elastic $np \rightarrow np$ differential cross section in the backward direction, i.e., at the incident neutron scattering angle $\theta_{\mathrm{CM}} = \pi$. The ratio of the two differential cross sections is then calculated.

The $np \rightarrow np$ differential cross section $(d\sigma/d\Omega)_{np}$ can be split into the «spin-independent» (SI) and «spin-dependent» (SD) parts:

$$\left(\frac{d\sigma}{d\Omega}\right)_{np} = \left(\frac{d\sigma}{d\Omega}\right)_{np}^{\mathrm{SI}} + \left(\frac{d\sigma}{d\Omega}\right)_{np}^{\mathrm{SD}}. \tag{1.1}$$

Following the mathematical formalism developed in [7–9], the differential cross section for $nd \rightarrow (nn) + p$ reaction in the framework of the impulse approximation (IA) can be written as

$$\left(\frac{d\sigma}{d\Omega}\right)_{nd} = [1 - F]\left(\frac{d\sigma}{d\Omega}\right)_{np}^{\mathrm{SI}} + \left[1 - \frac{1}{3}F\right]\left(\frac{d\sigma}{d\Omega}\right)_{np}^{\mathrm{SD}}. \tag{1.2}$$

Here F is the deuteron form factor, which is equal to the one in the backward direction [6]. The first term in the right-hand side of (1.2) vanishes, and for the differential cross section at $\theta_{\mathrm{CM}} = \pi$ the theory gives

$$\left(\frac{d\sigma}{d\Omega}\right)_{nd} = \frac{2}{3}\left(\frac{d\sigma}{d\Omega}\right)_{np}^{\mathrm{SD}}. \tag{1.3}$$

Only if IA holds, Eqs. (1.2) and (1.3) are valid.

We denote by $R_{\mathrm{QE}}(\theta_{\mathrm{CM}})$ the ratio of the quasi-elastic nd to the free np elastic scattering differential cross sections. From (1.3) it follows that

$$R_{\mathrm{QE}}(\pi) = \frac{(d\sigma/d\Omega)_{nd}}{(d\sigma/d\Omega)_{np}} = \frac{2}{3}\frac{(d\sigma/d\Omega)_{np}^{\mathrm{SD}}}{(d\sigma/d\Omega)_{np}} = R_{np}(\pi). \tag{1.4}$$

The observable $R_{\mathrm{QE}}(\pi)$ in the left-hand side is measured using the quasi-elastic result, whereas $R_{np}(\pi)$ is calculated from the known np amplitudes.

The ratio of the spin-independent to the spin-dependent part of $(d\sigma/d\Omega)_{np}$ at the same angle is

$$R_{np}^{\mathrm{ID}}(\pi) = \frac{(d\sigma/d\Omega)_{np}^{\mathrm{SI}}}{(d\sigma/d\Omega)_{np}^{\mathrm{SD}}} = \frac{2}{3R_{np}(\pi)} - 1. \tag{1.5}$$

Some authors use the ratio of the spin-independent part (SI) to the entire np elastic differential cross section. This ratio is

$$R_{np}^{\text{SI}}(\pi) = \frac{(d\sigma/d\Omega)_{np}^{\text{SI}}}{(d\sigma/d\Omega)_{np}} = \frac{2}{3} - R_{np}(\pi). \tag{1.6}$$

Another interesting quantity may also be the ratio of the spin-singlet part (SS) of the np differential cross section to $(d\sigma/d\Omega)_{np}$ at the angle π:

$$R_{np}^{\text{SS}}(\pi) = \frac{(d\sigma/d\Omega)_{np}^{\text{SS}}}{(d\sigma/d\Omega)_{np}}. \tag{1.7}$$

In Eqs. (1.5)–(1.7), the quantities for the np elastic scattering are given which can be taken from the phase shift analysis (PSA), if this analysis at a given energy exists. In Eqs. (1.5) and (1.6) the corresponding quantities, obtained using the quasi-elastic reaction, are to be labeled by QE. The desired equalities $R_{\text{QE}}(\pi) = R_{np}(\pi)$, $R_{\text{QE}}^{\text{ID}}(\pi) = R_{np}^{\text{ID}}(\pi)$ and $R_{\text{QE}}^{\text{SI}}(\pi) = R_{np}^{\text{SI}}(\pi)$ are to be checked.

A compatibility of the measured nd and np observables represents a check of the validity of the theory and its basic assumption (IA). If the theory and IA hold, the quasi-elastic quantity contributes to the phenomenological description of the elastic np system in the same manner as any other scattering observable. This concerns observables expressed by bilinear functions of amplitudes. Optical theorems provide more information. A knowledge of, e.g., $R_{\text{QE}}(\pi)$, even approximative, could then help in an unambiguous direct reconstruction of the np elastic scattering amplitudes (DRSA) analysis. The QE measured data and the np calculations using PSA could now be compared in the energy interval from 10 MeV to 1.3 GeV.

$R_{\text{QE}}(\pi)$ could be measured with proton, neutron and deuteron beams and with proton or deuteron targets, using either of the three reactions:

$$nd \rightarrow (nn) + p, \tag{1.8a}$$

$$pd \rightarrow (pp) + n, \tag{1.8b}$$

$$dp \rightarrow (pp) + n. \tag{1.8c}$$

Each reaction requires a specific experimental approach, and the measurements provide different systematic errors. In the charge-exchange scattering of the reactions (1.8a) and (1.8b), the remaining two nucleons (in brackets) are slow, within the Fermi-motion distribution. For the reaction (1.8c) the two outgoing protons in the laboratory system are relatively rapid and can be measured.

The reaction (1.8a) is investigated with a neutron beam, which is usually quasi-monochromatic. Outgoing fast protons are detected with $\sim 100\%$ efficiency. Their characteristics are well determined by a magnetic analysis, as well as by

TOF. At intermediate energies the charge-exchange proton distribution is well separate from the pion production region. A simple replacement of a deuteron target by a proton target allows one to measure both $(d\sigma/d\Omega)_{nd}$ and $(d\sigma/d\Omega)_{np}$ using the same beam line and set-up. For the ratio of these two differential cross sections, the normalization procedure is simplified to the knowledge of the deuterium and hydrogen contents in the targets. It is not surprising that the reaction (1.8a) was most frequently measured.

The reaction (1.8b) is measured with incident protons and with deuteron targets. The TOF measurement of the fast outgoing neutrons is crucial. The neutron detector efficiencies are small, and the absolute differential cross section is not easy to determine. The np elastic differential cross section measurement represents either a separate experiment or the necessary $(d\sigma/d\Omega)_{np}(\pi)$ value is to be obtained from another source.

The reaction (1.8c) is studied using accelerated incident deuterons and proton targets. The two remaining outgoing protons could be magnetically analyzed. This is often sufficient, even if the fast outgoing neutron is ignored. For measurements with an internal beam and a jet target (or a cell target), only this reaction could be performed. The $(d\sigma/d\Omega)_{np}(\pi)$ value again needs to be taken from another experiment. The reaction (1.8c) was used in the Dubna bubble chamber measurements only.

Inelastic contributions to the elastic and to any of the three quasi-elastic reactions differ considerably. The reactions (1.8a)–(1.8c) contain electromagnetic contributions, whereas the elastic np reaction is Coulomb-independent. Phillips [11] has shown that, although the different final-state interactions (FSI) between two low-energy neutrons in (1.8a) or two low-energy protons in (1.8b) give different shapes to the energy spectra of the fast nucleon in the two cases, the effect on the backward charge-exchange cross section is negligible. It is assumed that the same holds for the reaction (1.8c) [10].

In the past, the determination of $R_{QE}(\pi)$ was mainly considered as a contribution to our knowledge of the np system. When the polarized proton targets and the polarized neutron beams were available, many physicists preferred the measurements of the accessible spin-dependent np elastic scattering observables.

Nevertheless, the $R_{QE}(\pi)$ observable becomes interesting again, mainly for investigations of the Nd system and for its comparison with the np system. At JINR's VBLHE (Dubna) a high-quality quasi-monoenergetic polarized neutron beam was extracted in 1994 at the Synchrophasotron for the $\Delta\sigma_L(np)$ measurements [12–14]. This accelerator was stopped in 2005 and the polarized deuterons from the Nuclotron are still not available. On the other hand, intense unpolarized beams with very long spills were extracted. The DELTA–SIGMA set-up was completed by a spectometer, and the $R_{QE}(\pi)$ energy dependence was successfully extended up to 2.0 GeV [15].

New papers appeared in the field of the theory and phenomenology. Ladygina and Shebeko [16] studied the reaction (1.8c) for a description of pd break-up process. In their paper the influence of FSI on the differential cross section is also treated. The calculations in the framework of IA and the contribution of FSI for the DELTA–SIGMA experiment have recently been published by Ladygina [17]. Experiments at the Nuclotron are also prepared at the STRELA array, but measurements have not started yet.

Quasi-elastic experiments, complementary to those treated here (i.e., in the other hemisphere), were carried out at Saturne 2 using intense extracted polarized proton and deuteron beams. The powerful magnetic spectrometer SPES4 was used at high energies [18–20] and the spectrometer SPES1 at lower energies [21]. The theory is treated in [10, 22, 23].

Complementary experiments were carried out at COSY (Jülich), where the ANKE spectrometer has been installed. Using the internal proton beam and the deuterium cluster-jet target, the ANKE collaboration measured the differential cross section for the reaction (1.8b) with the forward emission of fast proton pairs [24]. The results were obtained at the proton energies $T_p = 0.6, 0.8, 0.95, 1.35$ and 1.9 GeV. The situation is very similar to that of backward elastic proton–deuteron scattering [27, 28]. In [16] the ANKE kinematics was treated.

In the work of Chiladze et al. [25] the ANKE collaboration is looking at a very soft process, where the neutron is just «tickled» a bit and comes out as a proton. The results obtained at the beam energy of vector and tensor polarized deuterons are equal to 1.17 GeV. The predictions at higher energies from [26] are also presented.

For the reaction (1.8b), using the internal polarized proton beam, the ANKE collaboration determined the analyzing power at $T_p = 0.5$ and 0.8 MeV. The CM angular region of emitted neutrons covers the interval from 167 to 180° [29]. The results demonstrate the $^1S_0$ wave dominance in the fast forward diproton formation. New experiments at COSY are to be expected.

In the present review, the expression of $R_{np}(\pi)$ as a function of amplitudes is given in five amplitude representations, frequently used in this field. In part of the relevant papers it is not defined, if the elastic scattering amplitudes concern the charge-exchange reaction $np \to pn$ at $\theta_{CM} = 0$ or the direct reaction $np \to np$ at $\theta_{CM} = \pi$. In Sec. 2 the observable $R_{np}(\pi)$ is expressed as a function of «invariant amplitudes» [30, 31]. This amplitude representation and formalism, as well as the four-index notation of experiments, have been used in all papers related to the DELTA–SIGMA JINR VBLHE experimental program. The same representation has been used in the NN program at Saturne 2, in the PSI experiments, in Gatchina, as well as in the papers of many other laboratories.

The expressions in helicity amplitudes [33], used in [34, 35], are compared with the invariant amplitude representation in Sec. 3. The Goldberger–Watson

amplitude representation [36], used, e.g., in [7,34,37], is treated in Sec. 4 and the singlet-triplet representation [38, 39], referred to in [40, 41], is shown in Sec. 5. The Wolfenstein amplitudes [42–45] are discussed in Sec. 6. The PSA predictions for $R_{np}(\pi)$ and for the other related observables are given in Sec. 7. Available experimental results for $R_{QE}(\pi)$ are listed in Sec. 8. They are discussed and compared with the calculated $R_{np}(\pi)$ energy dependence. The conclusions are drawn in Sec. 9.

2. INVARIANT AMPLITUDE REPRESENTATION

2.1. Direct Invariant Amplitudes. The nucleon–nucleon formalism, including the four-index notation and definition of all «pure» experiments, is described in [30]. The parity conservation, time reversal invariance as well as isospin invariance are assumed. The nucleon–nucleon elastic scattering matrix can be written in the form

$$M(\mathbf{k}_f, \mathbf{k}_i) = \frac{1}{2}[(a+b) + (a-b)(\boldsymbol{\sigma}_1, \mathbf{n})(\boldsymbol{\sigma}_2, \mathbf{n}) + (c+d)(\boldsymbol{\sigma}_1, \mathbf{m})(\boldsymbol{\sigma}_2, \mathbf{m}) +$$
$$+ (c-d)(\boldsymbol{\sigma}_1, \boldsymbol{\ell})(\boldsymbol{\sigma}_2, \boldsymbol{\ell}) + e(\boldsymbol{\sigma}_1 + \boldsymbol{\sigma}_2, \mathbf{n})], \quad (2.1)$$

where a, b, c, d and e are complex invariant amplitudes, which are functions of energy and scattering angle. The terms $\boldsymbol{\sigma}_1$ and $\boldsymbol{\sigma}_2$ are the Pauli 2×2 matrices for the beam and target particles, $\mathbf{k}_i$ and $\mathbf{k}_f$ are the unit vectors in the direction of the incident and final particles, respectively, and

$$\mathbf{n} = \frac{\mathbf{k}_i \mathbf{k}_f}{|\mathbf{k}_i \mathbf{k}_f|}, \quad \ell = \frac{\mathbf{k}_f + \mathbf{k}_i}{|\mathbf{k}_f + \mathbf{k}_i|}, \quad \mathbf{m} = \frac{\mathbf{k}_f - \mathbf{k}_i}{|\mathbf{k}_f - \mathbf{k}_i|}. \quad (2.2)$$

In [30] it is defined that the vector $\mathbf{k}_f$ is in the direction of the scattered particle, which is the same as the incident one. The scattering angle θ_{CM} is then the angle between $\mathbf{k}_i$ and $\mathbf{k}_f$. The «forward» or «backward» directions or the scattering angles $\theta_{CM} = 0$, π concern the final states of the beam particle.

The term $(a+b)$ in Eq. (2.1) is spin-independent (SI, sometimes called «spin non-flip term»), all the other terms are spin-dependent (SD, also called «spin-flip»). It should be noted that the spin-independent term is not the spin-singlet term, which is equal to $(b-c)$.

The scattering matrix simplifies at $\theta_{CM} = 0$ and π, where the vector $\mathbf{n}$ is not defined, since $\mathbf{k}_f = \mathbf{k}_i$ in the forward direction and $\mathbf{k}_f = -\mathbf{k}_i$ in the backward direction. The amplitudes in (2.2) then satisfy

$$a(0) - b(0) = c(0) + d(0), \quad e(0) = 0, \quad (2.3a)$$
$$a(\pi) - b(\pi) = c(\pi) - d(\pi), \quad e(\pi) = 0. \quad (2.3b)$$

The scattering matrices for pp, nn, np, and pn interactions are given in terms of isosinglet (M_0) and isotriplet (M_1) matrices, both of the form of Eq. (2.1). Putting

$$M(\mathbf{k}_f, \mathbf{k}_i) = \frac{M_0}{4}[1 - (\boldsymbol{\tau}_1, \boldsymbol{\tau}_2)] + \frac{M_1}{4}[3 + (\boldsymbol{\tau}_1, \boldsymbol{\tau}_2)], \qquad (2.4)$$

where $\boldsymbol{\tau}_1$ and $\boldsymbol{\tau}_2$ are the nucleon isospin matrices, we have

$$M(pp \to pp) = M(nn \to nn) = M_1, \qquad (2.5a)$$

$$M(np \to np) = M(pn \to pn) = \frac{1}{2}(M_1 + M_0), \qquad (2.5b)$$

$$M(np \to pn) = M(pn \to np) = \frac{1}{2}(M_1 - M_0). \qquad (2.5c)$$

Equations (2.5) hold also for individual scattering amplitudes, independently of their representation. One can write

$$\text{Ampl}\,(np) = \frac{1}{2}\Big(\text{Ampl}\,(I = 1) \pm \text{Ampl}\,(I = 0)\Big). \qquad (2.5d)$$

The sign in Eq. (2.5d) depends on a choice of Eq. (2.5b) or Eq. (2.5c). The matrix $M(np \to np)$ in Eq. (2.5b) describes the «direct elastic scattering» with the «direct scattering amplitudes».

The matrices M_1 and M_0 in Eqs. (2.5a)–(2.5c) are defined with the base vectors (2.2), where the vector $\mathbf{k}_f$ concerns the scattered particle, which is the same as the incident one. The matrix $M(np \to np)$ in Eq. (2.5b) describes the «direct elastic scattering» with the «direct scattering amplitudes». The matrix $M(np \to pn)$ in Eq. (2.5c) is called «charge-exchange (CEX) elastic scattering matrix», which has the same form as Eq. (2.1), but with the different base vectors and with the different CEX amplitudes. In the CEX system the vector $\mathbf{k}_f^{\text{CEX}}$ concerns the recoil particle, which is the target particle. With respect to the direct elastic scattering, the angle of the target particle changes from θ_{CM} to $\pi - \theta_{\text{CM}}$. The base vectors in Eq. (2.2c) change as follows:

$$\mathbf{n}_i^{\text{CEX}} = -\,\mathbf{n}, \quad \boldsymbol{\ell}^{\text{CEX}} = -\,\mathbf{m}, \quad \mathbf{m}^{\text{CEX}} = -\,\boldsymbol{\ell}. \qquad (2.6)$$

Since in the right-hand sides of all Eqs. (2.5) are the direct scattering amplitudes for $I = 1$ and $I = 0$, one can relate the CEX amplitudes in the left-hand side of Eqs. (2.5c) and (2.5d) to the direct ones. This procedure will be treated in Subsec. 2.2. In the present subsection the «forward» or «backward» scattering angles and directions concern the final state of the beam particle.

Symmetry conditions, shown in Table 1, connect the elastic scattering amplitudes a to e in Eq. (2.1) at θ_{CM} and at $\pi - \theta_{\text{CM}}$ for the given pure isospin states $I = 0$ and $I = 1$ [30, 32].

Table 1. **Symmetry properties of the NN scattering amplitudes**

$I = 0$ amplitudes	$I = 1$ amplitudes
$a_0(\theta) = +a_0(\pi - \theta)$	$a_1(\theta) = -a_1(\pi - \theta)$
$b_0(\theta) = +c_0(\pi - \theta)$	$b_1(\theta) = -c_1(\pi - \theta)$
$c_0(\theta) = +b_0(\pi - \theta)$	$c_1(\theta) = -b_1(\pi - \theta)$
$d_0(\theta) = -d_0(\pi - \theta)$	$d_1(\theta) = +d_1(\pi - \theta)$
$e_0(\theta) = -e_0(\pi - \theta)$	$e_1(\theta) = +e_1(\pi - \theta)$

The np elastic scattering differential cross section is given [30]:

$$\frac{d\sigma}{d\Omega} = \frac{1}{2}\big(|a|^2 + |b|^2 + |c|^2 + |d|^2 + |e|^2\big). \tag{2.7}$$

In the brackets one can also write

$$|a|^2 + |b|^2 = \frac{1}{2}(|a + b|^2 + |a - b|^2), \quad |c|^2 + |d|^2 = \frac{1}{2}(|c + d|^2 + |c - d|^2). \tag{2.8}$$

Using Eqs. (2.8) and (2.3a), in the forward direction ($\theta_{\mathrm{CM}} = 0$), one obtains

$$\left(\frac{d\sigma}{d\Omega}\right)(0) = \frac{1}{4}\big(|a(0) + b(0)|^2 + 2|a(0) - b(0)|^2 + |c(0) - d(0)|^2\big). \tag{2.9a}$$

In the backward direction ($\theta_{\mathrm{CM}} = \pi$), using (2.3b) instead of (2.3a), one has

$$\left(\frac{d\sigma}{d\Omega}\right)(\pi) = \frac{1}{4}\big(|a(\pi) + b(\pi)|^2 + 2|a(\pi) - b(\pi)|^2 + |c(\pi) + d(\pi)|^2\big). \tag{2.9b}$$

The expressions for the SI elastic differential cross sections at any angle have the same form:

$$\left(\frac{d\sigma}{d\Omega}\right)^{\mathrm{SI}}_{np \to np} = \frac{1}{4}\big(|a + b|^2\big). \tag{2.10}$$

Subtracting $(d\sigma/d\Omega)^{\mathrm{SI}}$ from Eq. (2.7), one obtains spin-dependent $(d\sigma/d\Omega)^{\mathrm{SD}}$. Its form is also independent of angle. Using Eq. (2.9a) or (2.9b), one has $(d\sigma/d\Omega)^{\mathrm{SD}}$ in the forward or in the backward directions, respectively.

For the ratio (1.6) in the backward direction holds

$$R^{\mathrm{SI}}_{np \to np}(\pi) = \frac{2}{3}\frac{\frac{1}{4}|a + b|^2}{\frac{1}{2}(|a|^2 + |b|^2 + |c|^2 + |d|^2)}. \tag{2.11}$$

Taking into account Eq. (2.3b), for Eq. (1.4) one obtains

$$R_{np \to np}(\pi) = \frac{2}{3} \frac{\frac{1}{4}|a-b|^2 + \frac{1}{2}(|c|^2 + |d|^2)}{\frac{1}{2}(|a|^2 + |b|^2 + |c|^2 + |d|^2)}. \tag{2.12}$$

For the ratio (1.5) holds

$$R_{np \to np}^{\text{ID}}(\pi) = \frac{\frac{1}{4}|a+b|^2}{\frac{1}{4}|a-b|^2 + \frac{1}{2}(|c|^2 + |d|^2)}. \tag{2.13}$$

All amplitudes in Eqs. (2.10) to (2.13) are to be considered at $\theta_{\text{CM}} = \pi$.

The spin-singlet differential cross section in Eq. (1.7) is

$$\left(\frac{d\sigma}{d\Omega}\right)_{np \to np}^{\text{SS}}(\pi) = \frac{1}{4}|b-c|^2. \tag{2.14}$$

The cross sections are often expressed as $d\sigma/dt$ or $d\sigma/du$, where the Mandelstam variables t and u are given:

$$t = -2P_{\text{CM}}^2(1 - \cos\theta_{\text{CM}}), \tag{2.15a}$$

$$u = -2P_{\text{CM}}^2(1 + \cos\theta_{\text{CM}}) + (M_1^2 - M_2^2)^2/E_{\text{CM}}^2. \tag{2.15b}$$

Here P_{CM} is the incident particle momentum in the CM system; M_1, M_2 are the beam and target particle masses, and $E_{\text{CM}} = \sqrt{M_1^2 + M_2^2 + 2T_1 M_2} = \sqrt{s}$ is the total CM energy. T_1 is the incident particle kinetic energy and s is the third Mandelstam variable. Throughout this review $M_1 = M_2$ is considered. Since

$$\frac{d\sigma}{d\Omega} = \frac{d\sigma}{dt}\frac{P_{\text{CM}}^2}{\pi} = \frac{d\sigma}{du}\frac{P_{\text{CM}}^2}{\pi} \tag{2.16}$$

is valid at any angle, the ratios (1.4) to (1.7) remain unaffected.

The general expression of the total cross section for a polarized nucleon beam, transmitted through a polarized proton target (PPT), with arbitrary directions of the beam and target polarizations, $\mathbf{P}_B$ and $\mathbf{P}_T$, respectively, was first deduced in [46,47]. Taking into account fundamental conservation laws, at $\theta_{\text{CM}} = 0$ it is written in the form

$$\sigma_{\text{tot}}(0) = \sigma_{0\text{tot}}(0) + \sigma_{1\text{tot}}(0)(\mathbf{P}_B, \mathbf{P}_T) + \sigma_{2\text{tot}}(0)(\mathbf{P}_B, \mathbf{k})(\mathbf{P}_T, \mathbf{k}), \tag{2.17}$$

where $\mathbf{k} = \mathbf{k}_i = \mathbf{k}_f$ is defined in Eq. (2.2). The term $\sigma_{0tot}(0)$ is the spin-independent total cross section (i.e., for unpolarized beam and target particles); σ_{1tot}, σ_{2tot} are the spin-dependent contributions. They are related to the measurable observables $\Delta\sigma_T(0)$ and $\Delta\sigma_L(0)$:

$$-\Delta\sigma_T(0) = 2\sigma_{1tot}(0), \qquad (2.18a)$$

$$-\Delta\sigma_L(0) = 2(\sigma_{1tot}(0) + \sigma_{2tot}(0)), \qquad (2.18b)$$

called «total cross section differences». The negative signs for $\Delta\sigma_T(0)$ and $\Delta\sigma_L(0)$) in Eqs. (2.18a), (2.18b) correspond to the usual, although unjustified, convention in the literature. The total cross section differences are measured with either parallel or antiparallel beam and target polarization directions. The polarization vectors are transversally oriented with respect to $\mathbf{k}$ for $\Delta\sigma_T(0)$ measurements and longitudinally oriented for $\Delta\sigma_L(0)$ experiments.

The NN formalism linearly relates $\sigma_{0tot}(0)$, $\Delta\sigma_T(0)$ and $\Delta\sigma_L(0)$ to the imaginary parts of the three independent forward scattering amplitudes $a(0)+b(0)$, $c(0)$ and $d(0)$ [30]:

$$\sigma_{0tot}(0) = \frac{2\pi}{K} \, \mathrm{Im} \, [a(0) + b(0)], \qquad (2.19a)$$

$$-\Delta\sigma_T(0) = \frac{4\pi}{K} \, \mathrm{Im} \, [c(0) + d(0)], \qquad (2.19b)$$

$$-\Delta\sigma_L(0) = \frac{4\pi}{K} \, \mathrm{Im} \, [c(0) - d(0)], \qquad (2.19c)$$

where $K = P_{CM}$ is the wave number (see Eq. (2.15)). Since at $\theta_{CM} = 0$ Eq. (2.3a) holds, all imaginary parts of amplitudes are known.

The real part of the SI term can be determined by the measurement of the elastic differential cross section at small angles. The extrapolation towards $\theta_{CM} = 0$ gives an estimation of the ratio [32]:

$$\rho(np \to np) = \frac{\mathrm{Re} \, (a(0) + b(0))}{\mathrm{Im} \, (a(0) + b(0))}. \qquad (2.20)$$

For np scattering the results are not very accurate. Another theoretical approach is to calculate the real parts of all independent amplitudes from their imaginary parts, through a dispersion relation analysis [48]. The $\rho(np)$ values were calculated by Kroll [49] up to 10 GeV (see graphs for $\rho(pp), \rho(np)$ and $\rho(I = 0)$ in [32]). They agree with the PSA results below 1.3 GeV. Similar calculations of the real parts of the spin-dependent amplitudes, also presented in [49], gave values which differ considerably from the more accurate PSA results. This is due to the fact that the first $\Delta\sigma_{T,L}^{np}$ data were not known until 1985.

With the exceptions of the three optical theorems, any other elastic scattering observable is determined as a bilinear combination of the real and/or imaginary

parts, where each term contains one complex and one complex-conjugate CM amplitudes.

Throughout this paper a four-subscript notation for all experimental quantities is used [30]. The subscripts of an observable X_{srbt} refer to the polarization states of the scattered, recoil, beam, and target particles, respectively. For the so-called «pure experiments» in the CM system, the polarizations of the incident and target particles are oriented along the basis vectors in Eq. (2.2). In the laboratory system the incident and target particle polarizations (last two subscripts) are oriented along the basis unit vectors

$$\mathbf{k} = \mathbf{k}_i, \mathbf{n}, \mathbf{s} = [\mathbf{nk}]. \tag{2.21a}$$

The scattered particles (first subscript) and the recoil particles (second subscript) are analyzed in the directions

$$\mathbf{k}', \mathbf{n}, \mathbf{s}' = [\mathbf{nk}'], \tag{2.21b}$$

$$\mathbf{k}'', \mathbf{n}, \mathbf{s}'' = [\mathbf{nk}'']. \tag{2.21c}$$

Here the unit vectors $\mathbf{k}'$ and $\mathbf{k}''$ are oriented along the directions of the scattered and the recoil particle momenta, respectively. The vector $\mathbf{n}$ in the CM and in the lab. systems is the same.

If the beam and/or target particles are unpolarized, or the polarization of a final particle is not analyzed, the corresponding label is set equal to zero. In this notation the differential cross section in Eq. (2.7) can be written as $(d\sigma/d\Omega) = I_{0000}$.

In principle, $4^4 = 256$ pure experiments can be defined as components of various tensors. If parity conservation, the generalized Pauli principle and time reversal invariance are assumed, the number of independent experiments is greatly reduced. Only 25 linearly independent quantities survive at any energy and angle. They determine 10 real and imaginary parts of scattering amplitudes. For DRSA, at any angle $0 < \theta_{\mathrm{CM}} < \pi$ one common phase remains unknown and the amplitudes are relative; i.e., they are determined with respect to one arbitrarily chosen real or imaginary part. Since the relations between amplitudes and observables are bilinear, each of the nine real numbers may have one ambiguity in sign. On the other hand, 18 (at most) arbitrary linearly independent observables always provide an unambiguous DRSA solution. It is also obvious that any amplitude combination can be expressed by $\leqslant 18$ linearly independent pure observables.

At $\theta_{\mathrm{CM}} = 0$ and π, DRSA provides absolute amplitudes, since their imaginary parts are unambiguously determined from Eqs. (2.19). In the following it is assumed that the $(I = 1)$ part of amplitudes is known and that the np amplitudes, splitted into the $(I = 1)$ and $(I = 0)$ parts (Eq. (2.5d)), can be transformed from $\theta_{\mathrm{CM}} = 0$ towards $\theta_{\mathrm{CM}} = \pi$ and vice versa, using Table 1. In the backward direction the np differential cross section (Eq. (2.7) or (2.9b)) is well known. The spin correlation parameters $A_{00nn}(np)$ and $A_{00kk}(np)$ are both measured in the

single scattering experiment with the polarized neutron beam and the polarized proton target. Moreover, they can be measured simultaneously with the np total cross section differences $-\Delta\sigma_T$ and $-\Delta\sigma_L$, respectively. The spin correlations are expressed as functions of amplitudes

$$\left(\frac{d\sigma}{d\Omega}\right) A_{00nn} = \frac{1}{2}\left(|a|^2 - |b|^2 - |c|^2 + |d|^2 + |e|^2\right), \tag{2.22a}$$

$$\left(\frac{d\sigma}{d\Omega}\right) A_{00kk} = -\operatorname{Re} a^\star d \ \cos\theta_{\mathrm{CM}} + \operatorname{Im} d^\star e \ \sin\theta_{\mathrm{CM}} + \operatorname{Re} b^\star c. \tag{2.22b}$$

Equations (2.22a) and (2.22b) hold at any angle. Using Eq. (2.3b) and a simple relation of the type

$$|a + d|^2 = |a|^2 + |d|^2 + 2\operatorname{Re} a^\star d, \tag{2.23}$$

at $\theta_{\mathrm{CM}} = \pi$ we get $|e|^2 = \operatorname{Im} d^\star e = \sin\pi = 0$, $\cos\pi = -1$ and

$$\frac{d\sigma}{d\Omega} \ (1 + A_{00kk}) = (b + c)^2, \tag{2.24}$$

$$\frac{d\sigma}{d\Omega} \ (1 - A_{00kk} - 2A_{00nn}) = (b - c)^2, \tag{2.25}$$

$$\frac{d\sigma}{d\Omega} \ (1 - A_{00kk} + 2A_{00nn}) = (2d - b - c)^2 = (-2a + b + c)^2. \tag{2.26}$$

This DRSA procedure was proposed in [50].

Three real parts may be determined with an independent sign ambiguity. Therefore, DRSA in the forward and backward direction at one energy gives eight possible solutions at most.

Any other independent non-zero observable, determined either in the forward or in the backward direction, or an additional constraint, decreases the global ambiguity by a factor of two [50]. To use the ratio $\rho(np)$ (Eq. (2.20)) and numerical values from [49] may help.

Some physicists believed that the observable R_{QE}, discussed above, could be used as an additional constraint at energies out of the np PSA interval. The comparison of the QE and np quantities will be shown in Sec. 8.

The expressions for several observables will be useful in the following, where the formulae calculated in [30] are used. For the polarizations of the outgoing particles and for the beam or target analyzing powers at any angle the following relation holds:

$$\left(\frac{d\sigma}{d\Omega}\right) P_{n000} = \left(\frac{d\sigma}{d\Omega}\right) P_{0n00} = \left(\frac{d\sigma}{d\Omega}\right) A_{00n0} = \left(\frac{d\sigma}{d\Omega}\right) A_{000n} = \operatorname{Re} a^\star e. \tag{2.27}$$

The observables from Eqs. (2.27) vanish at $\theta_{\mathrm{CM}} = 0$ and π. All the other observables listed below survive in the backward (and in the forward) direction.

The spin corelation coefficient A_{00ss} is expressed as

$$\left(\frac{d\sigma}{d\Omega}\right) A_{00ss} = +\mathrm{Re}\, a^\star d \cos\theta - \mathrm{Im}\, d^\star e \sin\theta + \mathrm{Re}\, b^\star c. \tag{2.28}$$

It is easy to show that in the forward and backward directions $A_{00ss} = A_{00nn}$. For this purpose, e.g., Eq. (2.22a) is to be written with the help of (2.23) as

$$\left(\frac{d\sigma}{d\Omega}\right) A_{00nn} = \frac{1}{2}\left(|a+d|^2 - \mathrm{Re}\, a^\star d - |b+c|^2 + \mathrm{Re}\, b^\star c\right), \tag{2.29}$$

and then, in the brackets to add and subtract $|a \pm d|^2 - |c+d|^2$. The sign depends on either Eq. (2.3a) or (2.3b), respectively.

The rescattering observables, measured with considerably smaller statistics, are the depolarization parameters. With labels as given in Eqs. (2.21), in the backward direction hold the relations

$$\left(\frac{d\sigma}{d\Omega}\right) D_{n0n0} = \left(\frac{d\sigma}{d\Omega}\right) D_{0n0n} = \frac{1}{2}\left(|a|^2 + |b|^2 - |c|^2 - |d|^2\right), \tag{2.30a}$$

$$\left(\frac{d\sigma}{d\Omega}\right) D_{k'0s0} = \left(\frac{d\sigma}{d\Omega}\right) D_{0s''0s} = +\mathrm{Re}\, a^\star b - \mathrm{Re}\, c^\star d, \tag{2.30b}$$

$$\left(\frac{d\sigma}{d\Omega}\right) D_{s'0k0} = \left(\frac{d\sigma}{d\Omega}\right) D_{0k''0k} = +\mathrm{Re}\, a^\star b + \mathrm{Re}\, c^\star d. \tag{2.30c}$$

Using a procedure similar to that in Eq. (2.29), one obtains $D_{k'0s0} = D_{0s''0s} = D_{0n0n}$.

Two depolarization parameters, labeled by spin components from Eqs. (2.2), give, e.g., in the backward direction

$$D_{\ell0\ell0} = D_{0\ell0\ell} = D_{k'0s0} = D_{0s''0s} = D_{n0n0} = D_{0n0n}, \tag{2.31a}$$

$$D_{m0m0} = D_{0m0m} = D_{s'0k0} = D_{0k''0k}. \tag{2.31b}$$

Finally, the expression for the polarization transfer parameter at $\theta_{\mathrm{CM}} = 0$ and π is given:

$$\left(\frac{d\sigma}{d\Omega}\right) K_{0nn0} = \left(\frac{d\sigma}{d\Omega}\right) K_{n00n} = \frac{1}{2}\left(|a|^2 - |b|^2 + |c|^2 - |d|^2\right). \tag{2.32}$$

The quantities $R_{np\to np}$, $R^{\mathrm{SI}}_{np\to np}$, $R^{\mathrm{SD}}_{np\to np}$ or $R^{\mathrm{SS}}_{np\to np}$, discussed above, cannot be labeled, since they are not pure experimental quantities. However, they can be expressed as combinations of the pure observables.

The quantity $(d\sigma/d\Omega)\, R^{\mathrm{SS}}_{np\to np}$, defined by Eq. (2.14), is 1/4 of the combination of three pure experimental quantities, as shown in Eq. (2.25). This

observable is linearly dependent on experiments planned to be measured within the DELTA–SIGMA program at the VBLHE Nuclotron.

The quantities $R_{np \to np}$, $R^{\mathrm{SI}}_{np \to np}$ and $R^{\mathrm{SD}}_{np \to np}$ are mutually linearly dependent. It is sufficient to express only one of them, e.g., $R^{\mathrm{SI}}_{np \to np}$, or the spin-independent backward differential cross section from Eq. (2.10). The sum of Eqs. (2.30a) and (2.7) gives

$$\left(\frac{d\sigma}{d\Omega} \right) (1 + D_{0n0n}) = \left(|a|^2 + |b|^2 \right) = |a + b|^2 - 2\mathrm{Re}\, a^\star b, \qquad (2.33)$$

in agreement with the rule (2.23).

The sum of Eqs. (2.30b) and (2.30c) gives $2\mathrm{Re}\, a^\star b$, which can be added to Eq. (2.33). From Eq. (2.10) one obtains

$$4 \left(\frac{d\sigma}{d\Omega} \right)^{\mathrm{SI}}_{np \to np} = \left(\frac{d\sigma}{d\Omega} \right)_{np} (1 + 2\, D_{0n0n} + D_{0k''0k}), \text{ or} \qquad (2.34\mathrm{a})$$

$$= \left(\frac{d\sigma}{d\Omega} \right)_{np} (1 + D_{0n0n} + D_{m0m0} + D_{\ell 0 \ell 0}), \text{ or} \qquad (2.34\mathrm{b})$$

$$= \left(\frac{d\sigma}{d\Omega} \right)_{np} (1 + D_{0n0n} + D_{0m0m} + D_{0\ell 0\ell}). \qquad (2.34\mathrm{c})$$

This observable, expressed by the combination of pure experimental quantities (two of them in (2.34b), (2.34c) are equal), gives independent information with respect to that contained in (2.24), (2.25) and (2.26.). If the theory of Chew and Pomeranchuk is valid, the measurement of one quasi-elastic reaction in Eqs. (1.8) would not only help to solve the sign ambiguity, but could fully contribute to DRSA. As will be seen below, this is not the case.

2.2. Charge-Exchange Invariant Amplitudes. In principle, no experiment can distinguish the elastic $np \to np$ scattering from the elastic charge-exchange (CEX) $np \to pn$ scattering at any angle. Kinematic characteristics of both final particles were measured wherever possible. Close to $\theta_{\mathrm{CM}} = 0$ or π the experiments are inclusive; i.e., for incident neutrons, either only the same scattered neutrons or only the outgoing protons are measured, respectively.

The convention to call the elastic np scattering the elastic charge-exchange at $\theta_{\mathrm{CM}} > 90°$, namely at very large angles, is to my mind not only unjustified, but unfortunate. For the NN interaction such terminology has been introduced probably by analogy with the π-nucleon scattering. This convention is irrelevant for the results of measurements, from the experimental point of view. The convention is also useless for the phenomenology of the NN elastic scattering. Of course, when using the CEX system, the signs, the subscripts and even the names of some pure observables change. The complete table of of the NN observables expressed in terms of the CEX scattering amplitudes in any representation does

not exist, since it would be useless. In the tables, compilations and databases generally used, the observables are written at the CM scattering angle, defined by the incident and the same final particle, scattered in the interval $0 \leqslant \theta_{\mathrm{CM}} \leqslant \pi$ (see, e.g., [30, 51, 53]). One could hardly imagine using this convention in PSA, or in any potential model, containing experimental data in the entire NN angular interval.

Some theoricians use the convention, e.g., to distinguish between different virtual meson exchanges, or for NN interaction models, valid in an restrained angular region. The advantages, if any, are negligible.

It is obvious that the value of any possible NN observable, pure or not, is independent of the choice of amplitude representation, i.e., also on the choice of direct or CEX systems. All the different representations are related linearly.

If two complete amplitude representations gave different results for an arbitrary observable, e.g., for $(d\sigma/d\Omega)^{\mathrm{SI}}$ or for $(d\sigma/d\Omega)^{\mathrm{SD}}$, one could declare the entire NN phenomenology to be wrong. Most physicists would agree that such eventuality is improbable.

Since in part of the relevant experimental papers it is not defined, if the elastic scattering amplitudes concern the CEX reaction $np \to pn$ at $\alpha_{\mathrm{CM}} = 0$ or the direct reaction $np \to np$ at $\theta_{\mathrm{CM}} = \pi$, below are shown the transformation relations between the CEX and direct systems in the invariant amplitude representation. Using Eq. (2.5c) (or Eq. (2.5d) with the sign «+») and the symmetry relations from Table 1, the CEX amplitudes in Eq. (2.5c) at $\alpha_{\mathrm{CM}} = \pi - \theta_{\mathrm{CM}}$ are given:

$$a^{np \to pn}(\alpha_{\mathrm{CM}}) = -a_1(\pi - \theta_{\mathrm{CM}}) - a_0(\pi - \theta_{\mathrm{CM}}) = -a^{np \to np}(\pi - \theta_{\mathrm{CM}}), \quad (2.35\mathrm{a})$$
$$b^{np \to pn}(\alpha_{\mathrm{CM}}) = -c_1(\pi - \theta_{\mathrm{CM}}) - c_0(\pi - \theta_{\mathrm{CM}}) = -c^{np \to np}(\pi - \theta_{\mathrm{CM}}), \quad (2.35\mathrm{b})$$
$$c^{np \to pn}(\alpha_{\mathrm{CM}}) = -b_1(\pi - \theta_{\mathrm{CM}}) - b_0(\pi - \theta_{\mathrm{CM}}) = -b^{np \to np}(\pi - \theta_{\mathrm{CM}}), \quad (2.35\mathrm{c})$$
$$d^{np \to pn}(\alpha_{\mathrm{CM}}) = +d_1(\pi - \theta_{\mathrm{CM}}) + d_0(\pi - \theta_{\mathrm{CM}}) = +d^{np \to np}(\pi - \theta_{\mathrm{CM}}), \quad (2.35\mathrm{d})$$
$$e^{np \to pn}(\alpha_{\mathrm{CM}}) = +e_1(\pi - \theta_{\mathrm{CM}}) + e_0(\pi - \theta_{\mathrm{CM}}) = +e^{np \to np}(\pi - \theta_{\mathrm{CM}}). \quad (2.35\mathrm{e})$$

Equations (2.3a) and (2.3b) for the CEX amplitudes at the angles $\alpha_{\mathrm{CM}} = 0$ and π will be

$$a^{\mathrm{CEX}}(0) + b^{\mathrm{CEX}}(0) = -c^{\mathrm{CEX}}(0) + d^{\mathrm{CEX}}(0), \quad e^{\mathrm{CEX}}(0) = 0, \qquad (2.36\mathrm{a})$$
$$a^{\mathrm{CEX}}(\pi) + b^{\mathrm{CEX}}(\pi) = -c^{\mathrm{CEX}}(\pi) - d^{\mathrm{CEX}}(\pi), \quad e^{\mathrm{CEX}}(\pi) = 0. \qquad (2.36\mathrm{b})$$

Since the entire differential cross section for the direct amplitudes (Eq. (2.7)) is a half-sum of the amplitudes squared, the expression for the CEX amplitudes is given by the same formula. Moreover, the following holds:

$$t^{\mathrm{CEX}} = -2P_{\mathrm{CM}}^2(1 - \cos\alpha_{\mathrm{CM}}) + (M_1^2 - M_2^2)^2/E_{\mathrm{CM}}^2, \qquad (2.37\mathrm{a})$$
$$u^{\mathrm{CEX}} = -2P_{\mathrm{CM}}^2(1 + \cos\alpha_{\mathrm{CM}}). \qquad (2.37\mathrm{b})$$

All variables are the same as in Eqs. (2.15). Putting again $M_1 = M_2$, one obtains

$$t^{\text{CEX}}(\alpha_{\text{CM}}) = u\ (\theta_{\text{CM}}), \quad u^{\text{CEX}}(\alpha_{\text{CM}}) = t(\theta_{\text{CM}}) \tag{2.38}$$

and

$$\left(\frac{d\sigma^{\text{CEX}}}{dt^{\text{CEX}}} \right) = \left(\frac{d\sigma^{\text{CEX}}}{du^{\text{CEX}}} \right) = \left(\frac{d\sigma}{dt} \right) = \left(\frac{d\sigma}{du} \right). \tag{2.39}$$

The spin-independent SI differential cross section at any angle in the CEX invariant amplitude representation is now given:

$$\left(\frac{d\sigma}{d\Omega} \right)^{\text{SI}}_{np \to pn} = \frac{1}{4} \left| a^{\text{CEX}} + c^{\text{CEX}} \right|^2. \tag{2.40}$$

One obtains the CEX spin-dependent $(d\sigma/d\Omega)^{\text{SD}}_{np \to pn}$ part by a subtraction of Eq. (2.40) from (2.7) at the same CEX angle. Its form is also the same at all angles.

For the ratio (1.6) at $\alpha_{\text{CM}} = 0$ holds

$$R^{\text{SI}}_{np \to pn}(\alpha = 0) = \frac{2}{3} \frac{\frac{1}{4} \left| a^{\text{CEX}} + c^{\text{CEX}} \right|^2}{\frac{1}{2} \left(\left| a^{\text{CEX}} \right|^2 + \left| b^{\text{CEX}} \right|^2 + \left| c^{\text{CEX}} \right|^2 + \left| d^{\text{CEX}} \right|^2 \right)}. \tag{2.41}$$

For Eq. (1.4) in the CEX system one obtains

$$R_{np \to pn}(\alpha = 0) = \frac{2}{3} \frac{\frac{1}{4} \left| a^{\text{CEX}} - c^{\text{CEX}} \right|^2 + \frac{1}{2} \left(\left| b^{\text{CEX}} \right|^2 + \left| d^{\text{CEX}} \right|^2 \right)}{\frac{1}{2} \left(\left| a^{\text{CEX}} \right|^2 + \left| b^{\text{CEX}} \right|^2 + \left| c^{\text{CEX}} \right|^2 + \left| d^{\text{CEX}} \right|^2 \right)}. \tag{2.42}$$

For the ratio (1.5), Eq. (2.13) is transformed into the CEX system as

$$R^{\text{ID}}_{np \to pn}(\alpha = 0) = \frac{\frac{1}{4} \left| a^{\text{CEX}} + c^{\text{CEX}} \right|^2}{\frac{1}{4} \left| a^{\text{CEX}} - c^{\text{CEX}} \right|^2 + \frac{1}{2} \left(\left| b^{\text{CEX}} \right|^2 + \left| d^{\text{CEX}} \right|^2 \right)}. \tag{2.43}$$

With the help of Eq. (2.14) the CEX spin-singlet differential cross section in Eq. (1.7) is expressed as

$$\left(\frac{d\sigma}{d\Omega} \right)^{\text{SS}}_{np \to pn} = \frac{1}{4} \left| b^{\text{CEX}} - c^{\text{CEX}} \right|^2, \tag{2.44}$$

at any angle α_{CM}.

The CEX amplitudes in Eqs. (2.40) to (2.44) are to be considered at $\alpha_{\mathrm{CM}} = 0$, i.e., at $\theta_{\mathrm{CM}} = \pi$. The transformation of the CEX amplitudes into the direct amplitudes and vice versa gives

$$R_{np \to pn}(\alpha_{\mathrm{CM}} = 0) = R_{np \to np}(\theta_{\mathrm{CM}} = \pi), \qquad (2.45a)$$

$$R_{np \to pn}^{\mathrm{SI}}(\alpha_{\mathrm{CM}} = 0) = R_{np \to np}^{\mathrm{SI}}(\theta_{\mathrm{CM}} = \pi), \qquad (2.45b)$$

$$R_{np \to pn}^{\mathrm{ID}}(\alpha_{\mathrm{CM}} = 0) = R_{np \to np}^{\mathrm{ID}}(\theta_{\mathrm{CM}} = \pi), \qquad (2.45c)$$

$$R_{np \to pn}^{\mathrm{SS}}(\alpha_{\mathrm{CM}} = 0) = R_{np \to np}^{\mathrm{SS}}(\theta_{\mathrm{CM}} = \pi). \qquad (2.45d)$$

The optical theorems in the CEX system are valid at $\alpha_{\mathrm{CM}} = \pi$, i.e., at $\theta_{\mathrm{CM}} = 0$ only. Equations (2.19) can be transformed as

$$\sigma_{0\mathrm{tot}}^{\mathrm{CEX}} = \frac{2\pi}{K} \, \mathrm{Im} \left[-a^{\mathrm{CEX}}(\alpha_{\mathrm{CM}} = \pi) - c^{\mathrm{CEX}}(\alpha_{\mathrm{CM}} = \pi) \right], \qquad (2.46a)$$

$$-\Delta\sigma_T^{\mathrm{CEX}} = \frac{4\pi}{K} \, \mathrm{Im} \left[-b^{\mathrm{CEX}}(\alpha_{\mathrm{CM}} = \pi) + d^{\mathrm{CEX}}(\alpha_{\mathrm{CM}} = \pi) \right], \qquad (2.46b)$$

$$-\Delta\sigma_L^{\mathrm{CEX}} = \frac{4\pi}{K} \, \mathrm{Im} \left[-b^{\mathrm{CEX}}(\alpha_{\mathrm{CM}} = \pi) - d^{\mathrm{CEX}}(\alpha_{\mathrm{CM}} = \pi) \right]. \qquad (2.46c)$$

The ratio of the real to imaginary part for CEX amplitudes is given:

$$\rho_{np \to pn}^{\mathrm{CEX}} = \frac{\mathrm{Re} \left(-a^{\mathrm{CEX}}(\alpha_{\mathrm{CM}} = \pi) - c^{\mathrm{CEX}}(\alpha_{\mathrm{CM}} = \pi) \right)}{\mathrm{Im} \left(-a^{\mathrm{CEX}}(\alpha_{\mathrm{CM}} = \pi) - c^{\mathrm{CEX}}(\alpha_{\mathrm{CM}} = \pi) \right)}. \qquad (2.47)$$

The relations (2.45) and (2.46) are written for illustrations only, since nobody will use them.

In the «CEX language» one uses the CEX amplitudes and the CEX CM base vectors from Eq. (2.6). The differential cross sections $(d\sigma/d\Omega)$ for CEX and direct amplitudes are given by the same formula, but at the conjugate angles. From the transformation relation (2.36) it can be seen that the polarizations and analyzing powers observables in Eq. (2.27) change signs:

$$A_{00,-n,0}^{\mathrm{CEX}}(\pi - \theta_{\mathrm{CM}}) = -A_{00n0}(\theta_{\mathrm{CM}}). \qquad (2.48a)$$

The spin correlation coefficient in Eq. (2.22a) is

$$A_{00,-n,-n}^{\mathrm{CEX}}(\pi - \theta_{\mathrm{CM}}) = A_{00nn}(\theta_{\mathrm{CM}}). \qquad (2.48b)$$

For the spin correlation coefficient in Eq. (2.22b) one obtains

$$A_{00kk}^{\mathrm{CEX}}(\pi - \theta_{\mathrm{CM}}) = A_{00kk}(\theta_{\mathrm{CM}}), \qquad (2.48c)$$

since $\cos(\pi - \theta_{\mathrm{CM}}) = -\cos\theta_{\mathrm{CM}}$ and $\sin(\pi - \theta_{\mathrm{CM}}) = +\sin\theta_{\mathrm{CM}}$.

Concerning Eqs. (2.30a) and (2.32), the corresponding CEX observables with respect to the direct ones even need to interchange their names:

$$D_{n0n0}^{\mathrm{CEX}}(\pi - \theta_{\mathrm{CM}}) = K_{0nn0}(\theta_{\mathrm{CM}}), \tag{2.48d}$$

$$K_{0nn0}^{\mathrm{CEX}}(\pi - \theta_{\mathrm{CM}}) = D_{n0n0}(\theta_{\mathrm{CM}}). \tag{2.48e}$$

The demonstration of the behaviour of other CEX observables witht respect to the direct observables may be interesting, but it is beyond the scope of the present review.

If the transformation relations between direct and CEX amplitudes are known for one amplitude representation, they can be easily written in any other representation. Only the transformation relations between the two amplitude representations, direct or CEX, are needed. Since any two amplitude representations are related linearly, the transformation of each pure observable or each combination of pure observables is always unambiguous.

3. HELICITY AMPLITUDE REPRESENTATION

The helicity amplitudes from [33] are denoted $\langle \lambda_3\ \lambda_4\ |M|\ \lambda_1\ \lambda_2 \rangle$, where M is the scattering matrix and $\lambda_1,\ \lambda_2,\ \lambda_3,\ \lambda_4$ are helicities for the beam, target, scattered and recoil particles in this order. The helicity λ for a nucleon is $1/2$ if the spin projection is parallel to the momentum, and $-1/2$ if it is antiparallel. The relations between the invariant amplitudes a, b, c, d, e and the five helicity amplitudes $\Phi_1, \Phi_2, \Phi_3, \Phi_4, \Phi_5$ are given in [30]:

$$\Phi_1 = \frac{1}{2}(+a\ \cos\theta_{\mathrm{CM}} + b - c + d + ie\ \sin\theta_{\mathrm{CM}}), \tag{3.1a}$$

$$\Phi_2 = \frac{1}{2}(+a\ \cos\theta_{\mathrm{CM}} - b + c + d + ie\ \sin\theta_{\mathrm{CM}}), \tag{3.1b}$$

$$\Phi_3 = \frac{1}{2}(+a\ \cos\theta_{\mathrm{CM}} + b + c - d + ie\ \sin\theta_{\mathrm{CM}}), \tag{3.1c}$$

$$\Phi_4 = \frac{1}{2}(-a\ \cos\theta_{\mathrm{CM}} + b + c + d - ie\ \sin\theta)_{\mathrm{CM}}, \tag{3.1d}$$

$$\Phi_5 = \frac{1}{2}(-a\ \sin\theta_{\mathrm{CM}} + ie\ \sin\theta_{\mathrm{CM}}). \tag{3.1e}$$

Formulae (3.1) can be inverted as

$$a = \frac{1}{2}[(+\Phi_1 + \Phi_2 + \Phi_3 - \Phi_4)\cos\theta_{\mathrm{CM}} - 4\Phi_5\sin\theta_{\mathrm{CM}}], \tag{3.2a}$$

$$b = \frac{1}{2}(+\Phi_1 - \Phi_2 + \Phi_3 + \Phi_4), \tag{3.2b}$$

$$c = \frac{1}{2}(-\Phi_1 + \Phi_2 + \Phi_3 + \Phi_4), \tag{3.2c}$$

$$d = \frac{1}{2}(+\Phi_1 + \Phi_2 - \Phi_3 + \Phi_4), \tag{3.2d}$$

$$e = \frac{1}{2}[(-\Phi_1 - \Phi_2 - \Phi_3 + \Phi_4)\sin\theta_{\mathrm{CM}} - 4\Phi_5\cos\theta_{\mathrm{CM}}]. \tag{3.2e}$$

At $\theta_{\mathrm{CM}} = 0$ holds

$$\Phi_4(0) = \Phi_5(0) = 0, \tag{3.3a}$$

and at $\theta_{\mathrm{CM}} = \pi$ one has

$$\Phi_3(\pi) = \Phi_5(\pi) = 0. \tag{3.3b}$$

This coincides with Eqs. (2.3a) and (2.3b).

The differential cross section in the helicity amplitude representation is given as

$$\frac{d\sigma}{d\Omega} = \frac{1}{2}\left(|\Phi_1|^2 + |\Phi_2|^2 + |\Phi_3|^2 + |\Phi_4|^2 + 4|\Phi_5|^2\right). \tag{3.4}$$

The expression for $R_{np}^{\mathrm{ID}}(\pi)$ is given as [35]

$$R_{np}^{\mathrm{ID}}(\pi) = \frac{|\Phi_4 - \Phi_2|^2}{2|\Phi_1|^2 + |\Phi_4 + \Phi_2|^2}. \tag{3.5}$$

Equation (1.5) provides

$$R_{np}(\pi) = \frac{2|\Phi_1|^2 + |\Phi_4 + \Phi_2|^2}{2|\Phi_1|^2 + |\Phi_4 + \Phi_2|^2 + |\Phi_4 - \Phi_2|^2}. \tag{3.6}$$

Using Eq. (2.8) the denominator of (3.6) can be written as

$$2|\Phi_1|^2 + |\Phi_4 + \Phi_2|^2 + |\Phi_4 - \Phi_2|^2 = 2(|\Phi_1|^2 + |\Phi_2|^2 + |\Phi_4|^2). \tag{3.7}$$

Substituting (3.1) and (3.3b) into (3.5) and (3.6), one expresses different terms as functions of the invariant amplitudes:

$$|\Phi_4 - \Phi_2|^2 = |a + b|^2, \tag{3.8a}$$
$$|\Phi_4 + \Phi_2|^2 = |c + d|^2, \tag{3.8b}$$
$$2|\Phi_1|^2 = |a - b|^2 + |c - d|^2, \tag{3.8c}$$

and for $R_{np}(\pi)$ and $R_{np}^{\mathrm{ID}}(\pi)$ one obtains the same expressions as Eqs. (2.9) and (2.10). The corresponding formulae in [35] are correct, whereas in [34] a misunderstanding occurs.

The spin-singlet amplitude is

$$b - c = \Phi_1 - \Phi_2, \tag{3.9}$$

and the spin-singlet differential cross section is easily found from Eq. (2.14). Since nobody uses the «CEX helicity amplitudes» they will be omitted here.

4. GOLDBERGER–WATSON AMPLITUDE REPRESENTATION

The Goldberger–Watson (GW) amplitudes [36] are labeled by index G in order to avoid a misunderstanding. The orthonormal vector basis (also in [34,37]) is identical with that given by Eqs. (2.2), and the operators $\boldsymbol{\sigma}_{1,2}$ are the same as in (2.1). The NN elastic scattering matrix is written as

$$M_G = a_G + b_G(\boldsymbol{\sigma}_1, \mathbf{n})(\boldsymbol{\sigma}_2, \mathbf{n}) + c_G[(\boldsymbol{\sigma}_1, \mathbf{n}) + (\boldsymbol{\sigma}_2, \mathbf{n})] +$$
$$+ e_G(\boldsymbol{\sigma}_1, \mathbf{m})(\boldsymbol{\sigma}_2, \mathbf{m}) + f_G(\boldsymbol{\sigma}_1, \boldsymbol{\ell})(\boldsymbol{\sigma}_2, \boldsymbol{\ell}). \quad (4.1)$$

The comparison of Eq. (4.1) with Eq. (2.1) gives

$$a_G = \frac{1}{2}(a+b), \quad b_G = \frac{1}{2}(a-b), \quad c_G = \frac{1}{2}e, \quad e_G = \frac{1}{2}(c+d), \quad f_G = \frac{1}{2}(c-d). \quad (4.2)$$

The differential cross section is given as

$$\frac{d\sigma}{d\Omega} = |a_G|^2 + |b_G|^2 + 2|c_G|^2 + |e_G|^2 + |f_G|^2. \quad (4.3)$$

Substituting Eqs. (4.2) into (4.3), one obtains Eq. (2.7).

The relations between Goldberger–Watson and helicity amplitudes are written for both $\theta_{\mathrm{CM}} = 0, \pi$. Using Eqs. (2.3a), (2.3b) and/or (3.3a), (3.3b), and indicating only the signs of the nucleon helicities, in the forward direction one has

$$a_G(0) = \frac{1}{2} (\Phi_1 + \Phi_3) = \frac{1}{2}(\langle ++, ++ \rangle + \langle +-, +- \rangle), \quad (4.4a)$$

$$b_G(0) = e_G(\pi) = \frac{1}{2} \Phi_2 = \frac{1}{2}(\langle ++, -- \rangle), \quad (4.4b)$$

$$c_G(0) = 0, \quad (4.4c)$$

$$f_G(0) = \frac{1}{2} (\Phi_3 - \Phi_1) = \frac{1}{2}(\langle +-, +- \rangle + \langle ++, ++ \rangle), \quad (4.4d)$$

which is given in [34].

For the backward np scattering the relations are

$$a_G(\pi) = \frac{1}{2}(\Phi_4 - \Phi_2) = \frac{1}{2}(\langle +-, -+ \rangle - \langle ++, -- \rangle), \quad (4.5a)$$

$$b_G(\pi) = f_G(\pi) = \frac{1}{2}\Phi_1 = \frac{1}{2}(\langle ++, ++ \rangle), \quad (4.5b)$$

$$c_G(\pi) = 0, \quad (4.5c)$$

$$e_G(\pi) = \frac{1}{2} (\Phi_2 + \Phi_4) = \frac{1}{2}(\langle ++, -- \rangle + \langle +-, -+ \rangle). \quad (4.5d)$$

The expressions $2|b_G| + |f_G|^2$ for the SD part and $|a|^2 + 2|b_G| + |f_G|^2$ for the entire differential cross section in [34,37,52] are again valid for the $np \to np$ forward scattering. In the backward direction the amplitude f_G needs to be replaced by the amplitude e_G.

If one introduces the mentioned corrections, for the discussed representation in the backward direction one has

$$R_{np}(\pi) = \frac{2}{3} \frac{2|b_G|^2 + |e_G|^2}{|a_G|^2 + 2|b_G|^2 + |e_G|^2}. \tag{4.6}$$

Putting Eqs. (4.2) into (4.6), one obtains Eq. (2.8).

The expressions for the SI and SD parts of the elastic scattering differential cross section in [34, 37] are written for the forward scattering of the incident particles. The same is repeated in [52] and in some recent unpublished reports from Jülich. The authors never used the available $np \to np$ elastic scattering amplitudes for their calculations.

The spin-singlet amplitude in the forward and the backward direction is

$$b - c = a_G - b_G - e_G - f_G. \tag{4.7}$$

One can apply either Eq. (4.4b) or Eq. (4.5b), depending on $\theta_{\mathrm{CM}} = 0, \ \pi$, respectively.

The optical theorems for this amplitude representation give

$$\sigma_{0\mathrm{tot}}(0) = \frac{2\pi}{K} \operatorname{Im} a_G(0), \tag{4.8a}$$

$$-\Delta\sigma_T(0) = \frac{4\pi}{K} \operatorname{Im} e_G(0), \tag{4.8b}$$

$$-\Delta\sigma_L(0) = \frac{4\pi}{K} \operatorname{Im} f_G(0). \tag{4.8c}$$

The ratio of the real to imaginary part is given by the SI term as

$$\rho(np) = \frac{\operatorname{Re} a_G(0)}{\operatorname{Im} a_G(0)}. \tag{4.9}$$

All quantities in (4.8) and (4.9) are given at $\theta_{\mathrm{CM}} = 0$.

The transformation formulae between the elastic scattering and the CEX Goldberger–Watson amplitudes are sometimes used. Then it is useful to express the CEX amplitudes given at $\alpha_{\mathrm{CM}} = 0$ by the direct amplitudes at $\theta_{\mathrm{CM}} = \pi$. The transformation relations are

$$a_G^{\mathrm{CEX}}(0) = -\frac{1}{2} \big(a_G(\pi) + 2b_G(\pi) + e_G(\pi) \big), \tag{4.10a}$$

$$b_G^{\mathrm{CEX}}(0) = -\frac{1}{2} \big(a_G(\pi) + e_G(\pi) \big), \tag{4.10b}$$

$$e_G^{\mathrm{CEX}}(0) = -\frac{1}{2} \big(a_G(\pi) - 2b_G(\pi) + e_G(\pi) \big). \tag{4.10c}$$

The inverted relations are symmetric:

$$a_G(\pi) = -\frac{1}{2}\big(a_G^{\text{CEX}}(0) + 2b_G^{\text{CEX}}(0) + e_G^{\text{CEX}}(0)\big), \tag{4.11a}$$

$$b_G(\pi) = -\frac{1}{2}\big(a_G^{\text{CEX}}(0) + e_G^{\text{CEX}}(0)\big), \tag{4.11b}$$

$$e_G(\pi) = -\frac{1}{2}\big(a_G^{\text{CEX}}(0) - 2b_G^{\text{CEX}}(0) + e_G^{\text{CEX}}(0)\big). \tag{4.11c}$$

For the transformation formulae between the CEX amplitudes in the Goldberger–Watson representation and the direct invariant amplitude representation, the formulae (4.2) are to be substituted into Eqs. (4.10):

$$a_G^{\text{CEX}}(\alpha_{\text{CM}} = 0) = -\frac{1}{2}\big(a(\theta_{\text{CM}} = \pi) + c(\theta_{\text{CM}} = \pi)\big), \tag{4.12a}$$

$$b_G^{\text{CEX}}(\alpha_{\text{CM}} = 0) = -\frac{1}{2}\big(a(\theta_{\text{CM}} = \pi) - c(\theta_{\text{CM}} = \pi)\big), \tag{4.12b}$$

$$e_G^{\text{CEX}}(\alpha_{\text{CM}} = 0) = -\frac{1}{2}\big(b(\theta_{\text{CM}} = \pi) + d(\theta_{\text{CM}} = \pi)\big). \tag{4.12c}$$

Comparing, e.g., Eqs. (2.41) and (4.12a), one concludes that the spin-independent parts of the differential cross sections are identical.

5. SINGLET-TRIPLET AMPLITUDE REPRESENTATION

This representation has been developed and exhaustively described by Stapp [38]. It was successfully used in PSA of Stapp, Ypsilantis and Metropolis [39]. The vector basis is the same as given by Eqs. (2.2). The scattering matrix elements M_{if} are CM amplitudes with $i, f = 1, 0, -1$ indicating initial and final spin projections in the spin-triplet system and $i = f = S$ indicating the spin-singlet amplitude. The angle θ is given in the CM system. The transformation relations are

$$M_{\text{SS}} = b - c, \quad M_{00} = a + d\cos\theta, \quad M_{11} = \frac{1}{2}(a + b + c - d\cos\theta),$$

$$M_{10} = -\frac{1}{\sqrt{2}}(d\sin\theta + ie), \quad M_{01} = -\frac{1}{\sqrt{2}}(d\sin\theta - ie),$$

$$\tag{5.1}$$

$$M_{1-1} = \frac{1}{2}(-a + b + c + d\cos\theta) = M_{11} - M_{00} - \sqrt{2}\,(M_{10} + M_{01})\cotan\theta,$$

$$M_{-1-1} = M_{11}, \quad M_{-11} = M_{1-1}, \quad M_{0-1} = M_{01}, \quad M_{-10} = -M_{10},$$

which implies

$$a = \frac{1}{2}(M_{11} + M_{00} - M_{1-1}),$$

$$b = \frac{1}{2}(M_{11} + M_{SS} + M_{1-1}),$$

$$c = \frac{1}{2}(M_{11} - M_{SS} + M_{1-1}), \tag{5.2}$$

$$d = \frac{1}{2\cos\theta}(-M_{11} + M_{00} + M_{1-1}) = -\frac{1}{\sqrt{2}\sin\theta}(-M_{10} + M_{01}),$$

$$e = \frac{1}{\sqrt{2}}(M_{10} - M_{01}).$$

The differential cross section in this representation [38, 39] is

$$\frac{d\sigma}{d\Omega} = \frac{1}{4}|M_{SS}|^2 + \frac{1}{4}|M_{00}|^2 + \frac{1}{2}|M_{11}|^2 + \frac{1}{2}|M_{10}|^2 + \frac{1}{2}|M_{01}|^2 + \frac{1}{2}|M_{1-1}|^2. \tag{5.3}$$

Its spin-singlet and spin-triplet parts are separated at any angle.

In the forward as well as in the backward directions only three amplitudes survive, and

$$M_{10} = M_{01} = M_{1-1} = 0$$

in agreement with Eqs. (2.3a) and (2.3b). Then Eq. (5.3) contains the first three quadratical terms in the right-hand side only and Eq. (1.7) becomes very simple. From the three mutually related ratios (1.4) to (1.6) the simplest expression is that for $R_{np}^{SI}(\pi)$, where

$$\left(\frac{d\sigma}{d\Omega}\right)_{np}^{SI} = \frac{1}{4}\left(M_{11} + \frac{1}{2}M_{00} + \frac{1}{2}M_{SS}\right)^2. \tag{5.4}$$

In [41] the corresponding formulae are correct. In [40] there is a mistake in the expression of $(d\sigma/d\Omega)_{np}$ at $\theta_{CM} = 0, \pi$.

6. WOLFENSTEIN AMPLITUDE REPRESENTATION

The Wolfenstein amplitudes B, C, N, G, H [42–45] were often used by the JINR theoricians. The orthonormal vector basis is identical with that given by Eqs. (2.2) and the operators $\boldsymbol{\sigma}_{1,2}$ are the same as in (2.1). The NN elastic

scattering matrix is written as

$$M_{\mathbf{k}_f, \mathbf{k}_i} = B\hat{S} + \Big(C(\boldsymbol{\sigma}_1 + \boldsymbol{\sigma}_2, \mathbf{n}) + N(\boldsymbol{\sigma}_1, \mathbf{n})(\boldsymbol{\sigma}_2, \mathbf{n}) +$$
$$+ \frac{1}{2} G \left[(\boldsymbol{\sigma}_1, \mathbf{m})(\boldsymbol{\sigma}_2, \mathbf{m}) + (\boldsymbol{\sigma}_1, \boldsymbol{\ell})(\boldsymbol{\sigma}_2, \boldsymbol{\ell}) \right] +$$
$$+ \frac{1}{2} H \left[(\boldsymbol{\sigma}_1, \mathbf{m})(\boldsymbol{\sigma}_2, \mathbf{m}) - (\boldsymbol{\sigma}_1, \boldsymbol{\ell})(\boldsymbol{\sigma}_2, \boldsymbol{\ell}) \right] \Big) \hat{T}, \quad (6.1)$$

where $\hat{S}$ and $\hat{T}$ are the spin-singlet and spin-triplet projection operators, respectively:

$$\hat{S} = \frac{1}{4} \big(1 - (\boldsymbol{\sigma}_1, \boldsymbol{\sigma}_2) \big), \quad \hat{T} = \frac{1}{4} \big(3 + (\boldsymbol{\sigma}_1, \boldsymbol{\sigma}_2) \big). \qquad (6.2)$$

The Wolfenstein amplitudes are related to the invariant amplitudes as

$$B = (b - c), \quad C = e/2, \quad N = a, \quad G = a + b + c, \quad H = d, \qquad (6.3a)$$

which implies

$$a = N, \quad b = \frac{B - G + N}{2}, \quad c = \frac{G - B - N}{2}, \quad d = H, \quad e = 2C. \qquad (6.3b)$$

The Wolfenstein CEX amplitudes can be written by substituting Eqs. (2.35) into (6.3a).

7. ENERGY DEPENDENCE OF np OBSERVABLES

The energy dependence of $(d\sigma/d\Omega)_{np}$, $(d\sigma/d\Omega)_{np}^{\mathrm{SD}}$, $(d\sigma/d\Omega)_{np}^{\mathrm{SI}}$, $(d\sigma/d\Omega)_{np}^{\mathrm{SS}}$ and the ratios (1.4) to (1.7) for the $np \to np$ elastic reaction can be calculated using scattering amplitudes determined by PSA. In what follows, used are the Energy Dependent (ED) George Washington University and Virginia Polytechnic Institute (GW/VPI) PSA of Arndt, Strakovsky and Workman [53], solution SP04, the fixed energy solutions (FE) GW/VPI PSA, SES solution SP05 and FE Saclay-Geneva (SG) PSA [54], solutions 2007.

The energy interval, where GW/VPI PSA could be carried out, reaches 1.3 GeV (2.03 GeV/c) for np scattering, but the spin-dependent data above 1.1 GeV are rare. The PSA for pp scattering can be used up to 3.0 GeV, but there is a lack of data above 2.7 GeV. ED GW/VPI PSA cannot calculate the errors of any observable due to its energy dependence. The amplitudes in FE GW/VPI PSA are also determined without errors.

The SG PSA could be carried out up to 1.1 GeV (1.81 GeV/c) for np scattering and up to 2.7 GeV for pp scattering. Errors are calculated as square roots of the error matrix diagonal elements. The comparison of results shows a good agreement between the PSA results for all observables.

PSA uses all measured observables, either spin-independent or spin-dependent. PSA provides most complete information, which is practically model-independent, and no better tool for the prediction of any observable behaviour is available.

Several authors declared that «The existing data on np reaction are still very scanty and concern mainly the differential cross section distributions». Such a statement was true in 1975 (see [34]), when only np analyzing power data were measured at high energy (LBL, ANL, and CERN). No np two-spin experiments above 635 MeV existed. The neutron–proton PSA was possible below the Dubna synchrocyclotron energy only.

It is surprising that this statement is repeated, e.g., in [37] published in 2002. In very recent reports of the ANKE collaboration, the same declarations appear, whereas many sources provide information how the np database has changed. For example, the SAID database [53] or the Durham University (UK) data collections are accessible for everybody. Let me now summarize the present status of the np database at intermediate energies.

About 2000 spin-dependent np elastic scattering data points, concerning 11 to 13 independent observables, were determined at Saturne 2, mainly between 0.8 and 1.1 GeV in large angular intervals. These data were collected in [55] and later completed [56]. A comparable amount of np data in the region from 0.5 to 0.8 GeV was measured at LAMPF, and in the energy interval from 0.2 to 0.56 GeV at PSI. The amount of the np data below 0.5 GeV from TRIUMF cannot be neglected. The Saturne 2 and the PSI data were sufficient not only for the PSA procedure, but allowed one to perform the DRSA analysis at several energies and angles. It appears that the spin-dependent data are more or less sufficient, whereas above 0.8 GeV here is a lack of np differential cross section data, mainly at medium angles. This fact is in contradiction with the statement in [37]. Let me note that the lack of $(d\sigma/d\Omega)_{np}$ can be overcome better by ED PSA than by PSA at fixed energies, since the energy dependence of the data plays an important role.

Table 2 shows the relevant np observables in a large energy interval, calculated from ED GW/VPI PSA at $\theta_{\mathrm{CM}} = \pi$. In Fig. 1 are plotted the $(d\sigma/d\Omega)_{np}(\pi)$ and $(d\sigma/d\Omega)_{np}^{\mathrm{SD}}$ cross sections, in Fig. 2 are shown $(d\sigma/d\Omega)_{np}^{\mathrm{SI}}$ and $(d\sigma/d\Omega)_{np}^{\mathrm{SS}}$ together with the results from both FE PSA. In Figs. 3–5 are shown the $R_{np}(\pi)$, $R_{np}^{\mathrm{ID}}(\pi)$ and $R_{np}^{\mathrm{SS}}(\pi)$ observables, respectively, calculated from the three mentioned PSA. The comparison with measured quasi-elastic points listed in Tables 3–5 and also shown in Figs. 3 and 4 will be discussed in Sec. 8.

Table 2. **Values of** $(d\sigma/d\Omega)_{np}$, $(d\sigma/d\Omega)_{np}^{\text{SD}}$, $(d\sigma/d\Omega)_{np}^{\text{SS}}$, R_{np}, R_{np}^{ID} **and** R_{np}^{SS} **at** $\theta_{\text{CM}} = \pi$ **calculated from the energy-dependent PSA of Arndt et al.**

T_{kin}, GeV	$\left(\dfrac{d\sigma}{d\Omega}\right)_{np}$, mb/sr	$\left(\dfrac{d\sigma}{d\Omega}\right)_{np}^{\text{SD}}$, mb/sr	$\left(\dfrac{d\sigma}{d\Omega}\right)_{np}^{\text{SS}}$, mb/sr	R_{np}	R_{np}^{ID}	R_{np}^{SS}
0.010	78.750	11.875	19.514	0.101	5.632	0.165
0.020	42.910	6.152	11.681	0.096	5.975	0.272
0.030	29.830	4.489	9.461	0.100	5.645	0.317
0.050	20.090	3.348	8.173	0.111	5.001	0.407
0.070	16.690	3.004	7.947	0.120	4.556	0.476
0.100	14.650	2.930	8.182	0.133	4.000	0.558
0.120	13.950	2.907	8.365	0.139	3.798	0.600
0.150	13.250	3.008	8.620	0.151	3.405	0.651
0.200	12.440	3.240	8.902	0.174	2.839	0.716
0.250	11.860	3.507	9.054	0.197	2.382	0.763
0.300	11.430	3.839	9.170	0.224	1.977	0.802
0.350	11.170	4.222	9.356	0.252	1.646	0.838
0.380	11.070	4.481	9.470	0.270	1.471	0.856
0.400	11.010	4.658	9.541	0.282	1.358	0.867
0.450	10.860	5.106	9.678	0.313	1.127	0.891
0.500	10.610	5.485	9.642	0.345	0.935	0.909
0.550	10.090	5.569	9.266	0.368	0.812	0.918
0.600	9.448	5.629	8.638	0.397	0.678	0.914
0.650	9.082	5.542	8.147	0.406	0.644	0.897
0.700	8.996	5.384	7.871	0.399	0.671	0.875
0.750	8.998	5.185	7.698	0.384	0.735	0.856
0.800	8.991	4.955	7.551	0.367	0.817	0.840
0.850	8.960	4.717	7.410	0.351	0.900	0.827
0.900	8.909	4.486	7.267	0.336	0.986	0.816
0.950	8.849	4.271	7.134	0.322	1.072	0.806
1.000	8.786	4.074	7.010	0.309	1.157	0.798
1.050	8.726	3.900	6.905	0.298	1.237	0.791
1.100	8.673	3.753	6.820	0.289	1.311	0.786
1.150	8.633	3.630	6.753	0.280	1.371	0.782
1.200	8.610	3.544	6.653	0.274	1.434	0.774
1.250	8.610	3.402	6.696	0.263	1.527	0.778
1.300	8.636	3.431	6.701	0.265	1.517	0.776

Looking at the values in Table 2 and at the curves in Figs. 1 and 2, one observes that within the investigated energy interval the spin-independent part $(d\sigma/d\Omega)_{np}^{\text{SI}}$ decreases rapidly with increasing energy, reaches a minimum around 650 MeV and then slowly increases. This part is predicted to be dominant below

Fig. 1. The np elastic differential cross sections and its SD parts at $\theta_{CM} = \pi$. The curves are calculated from ED GW/VPI PSA [53] (sol. SP04). Curve 1 — $(d\sigma/d\Omega)_{np}$, curve 2 — $(d\sigma/d\Omega)_{np}^{SD}$, diamonds — $(d\sigma/d\Omega)_{np}(el)$ from GW/VPI PSA [53] SES (sol. SP05), open triangles — $(d\sigma/d\Omega)_{np}^{SD}$ from the same PSA, empty stars — $(d\sigma/d\Omega)_{np}(el)$ from Saclay-Geneva (SG) PSA [54] (solutions 2007), black stars — $(d\sigma/d\Omega)_{np}^{SD}$ from SG PSA
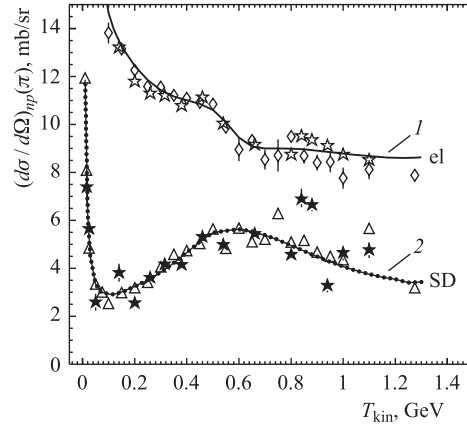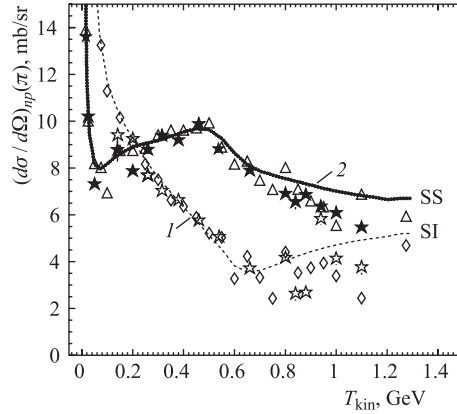
Fig. 2. The SI and SS np differential cross sections at $\theta_{CM} = \pi$. The curves are calculated from ED GW/VPI PSA [53] (sol. SP04). Curve 1 — $(d\sigma/d\Omega)_{np}^{SI}$, curve 2 — $(d\sigma/d\Omega)_{np}^{SS}$. Other symbols are the same as in Fig. 1

450 MeV, as expected. It also seems to be dominant above 900 MeV. The spin-dependent part $(d\sigma/d\Omega)_{np}^{SD}$ reaches a weak maximum around 600 MeV and slowly decreases towards the high energy. The spin-singlet cross section $(d\sigma/d\Omega)_{np}^{SS}$ is an essential part of the entire np elastic cross section above 200 MeV.

8. MEASURED QUASI-ELASTIC OBSERVABLES

The quasi-elastic experiments started at UCRL, Berkeley (University of California Radiation Laboratory, later LRL, now LBL), in Harvard University, Cambridge Massachusetts, and at the Institute of Nuclear Problems in Dubna (former INP Dubna, now JINR).

The first measurement of the differential cross section of the nd reaction was carried out at UCRL by Powell in 1951 [57]. The data at 90 MeV were

reported in [2], being given on the graph only. The estimated result is $R_{\mathrm{QE}}(\pi) = 0.397 \pm 0.044$. One year later a new result was published by Cladis, Hadley and Hess [58]. The experiment has been performed at the synchrocyclotron of UCRL using 270 MeV neutron beam. The authors obtained $R_{\mathrm{QE}}(\pi) = 0.710 \pm 0.021$ (the weighted average error in [58] is given as ± 0.201 by misprint and is repeated in [52]). The experiments [57,58] used the reaction (1.8a). In 1953 Hofmann and Strauch [59] published results on the interaction of 95 MeV protons with several nuclei (reaction (1.8b)). Measurements were carried out at the Harvard University accelerator. An estimation from the plotted data gives $R_{\mathrm{QE}}(\pi) = 0.48 \pm 0.03$.

At the Dubna synchrocyclotron the first measurements were carried out by Dzhelepov, Kazarinov, Golovin, Flyagin and Satarov [60, 61] in 1952–1954

Table 3. **The $R_{\mathrm{QE}}(\pi)$ and $R_{\mathrm{QE}}^{\mathrm{ID}}(\pi)$ data measured using the reaction (1.8a). The uncertainties are total errors**

T_{kin}, MeV	$R_{\mathrm{QE}}(\pi)$	$R_{\mathrm{QE}}^{\mathrm{ID}}(\pi)$	Laboratory	Year	Ref.
13.9	0.185	+2.604	Moscow	1965	[64]
90.0	0.397 ± 0.044	$+0.679 \pm 0.186$	UCRL	1951	[57]
152.0	0.650 ± 0.100	$+0.026 \pm 0.158$	Harvard U.	1966	[65]
200.0	0.553 ± 0.030	$+0.206 \pm 0.065$	JINR DLNP	1962	[63]
270.0	0.710 ± 0.021	-0.061 ± 0.028	UCRL	1952	[58]
299.7	0.652 ± 0.033	$+0.023 \pm 0.051$	PSI	1988	[52]
319.8	0.643 ± 0.032	$+0.037 \pm 0.052$	PSI	1988	[52]
339.7	0.637 ± 0.032	$+0.047 \pm 0.053$	PSI	1988	[52]
359.6	0.626 ± 0.031	$+0.065 \pm 0.053$	PSI	1988	[52]
379.6	0.641 ± 0.032	$+0.040 \pm 0.053$	PSI	1988	[52]
380.0	0.200 ± 0.035	$+2.333 \pm 0.583$	INP Dubna	1955	[60]
399.7	0.610 ± 0.031	$+0.093 \pm 0.055$	PSI	1988	[52]
419.8	0.623 ± 0.031	$+0.070 \pm 0.033$	PSI	1988	[52]
440.0	0.630 ± 0.032	$+0.058 \pm 0.053$	PSI	1988	[52]
460.1	0.611 ± 0.031	$+0.091 \pm 0.055$	PSI	1988	[52]
480.4	0.608 ± 0.030	$+0.097 \pm 0.054$	PSI	1988	[52]
500.9	0.592 ± 0.030	$+0.126 \pm 0.057$	PSI	1988	[52]
521.1	0.604 ± 0.030	$+0.104 \pm 0.055$	PSI	1988	[52]
539.4	0.617 ± 0.031	$+0.081 \pm 0.054$	PSI	1988	[52]
550.0	0.564 ± 0.039	$+0.182 \pm 0.084$	JINR VBLHE	2007	
557.4	0.632 ± 0.032	$+0.055 \pm 0.053$	PSI	1988	[52]
710.0	0.483 ± 0.080	$+0.380 \pm 0.229$	LRL	1960	[62]
794.0	0.560 ± 0.040	$+0.191 \pm 0.085$	LAMPF	1978	[41]
800.0	0.546 ± 0.035	$+0.212 \pm 0.078$	JINR VBLHE	2006	[15]
1000	0.567 ± 0.024	$+0.175 \pm 0.050$	JINR VBLHE	2006	[15]
1200	0.551 ± 0.022	$+0.210 \pm 0.048$	JINR VBLHE	2006	[15]
1400	0.562 ± 0.036	$+0.187 \pm 0.075$	JINR VBLHE	2006	[15]
1800	0.515 ± 0.032	$+0.296 \pm 0.081$	JINR VBLHE	2006	[15]
2000	0.506 ± 0.030	$+0.317 \pm 0.077$	JINR VBLHE	2006	[15]

with the neutron beam of 380 MeV. The value of $R_{\mathrm{QE}}(\pi) = 0.200 \pm 0.035$ was obtained. The authors mentioned [57, 58], two of the three previous papers, and considered that the Dubna experimental point and the UCRL data are compatible.

In 1960 Larsen [62] at LRL, Berkeley, measured the same quantity at relatively high energy of 710 MeV and obtained $R_{\mathrm{QE}}(\pi) = 0.483 \pm 0.080$. In his publication no previous result was mentioned.

Dzhelepov, in his contribution to the 1962 CERN conference [63], presented angular dependence of $R_{\mathrm{QE}}(\theta)$ at 200 MeV. He declared that the authors of this experiment are Yu. Kazarinov, V. Kiselev and Yu. Simonov, but no reference was given. Reading the value from the graph, one obtains $R_{\mathrm{QE}}(\pi) = 0.553 \pm 0.030$.

The accessible existing data, measured using the reactions (1.8a), (1.8b) and (1.8c), are given in Tables 3, 4 and 5, respectively. In the tables are listed the kinetic energy, $R_{\mathrm{QE}}(\pi)$ and $R_{\mathrm{QE}}^{\mathrm{ID}}(\pi)$ experimental values and errors, laboratory, year of publication and reference. Several papers give the numerical values of $R_{\mathrm{QE}}^{\mathrm{ID}}(\pi)$. Other articles show the $(d\sigma/d\Omega)_{\mathrm{QE}}$ angular distribution or give the charge-exchange value only. In such cases, the final ratios $R_{\mathrm{QE}}(\pi)$ and $R_{\mathrm{QE}}^{\mathrm{ID}}(\pi)$ listed here were obtained using $(d\sigma/d\Omega)_{np}(\pi)$ from ED GW/VPI PSA (solution SP04), shown in Table 2.

Table 4. **The** $R_{\mathrm{QE}}(\pi)$ **and** $R_{\mathrm{QE}}^{\mathrm{ID}}(\pi)$ **data measured using the reaction (1.8b).** **The uncertainties are total errors**

T_{kin}, MeV	$R_{\mathrm{QE}}(\pi)$	$R_{\mathrm{QE}}^{\mathrm{ID}}(\pi)$	Laboratory	Year	Ref.
13.5	0.180	+2.704	Livermore	1959	[66]
30.1	0.141 ± 0.035	$+3.728 \pm 1.174$	Rutherford	1967	[67]
50.0	0.240 ± 0.060	$+1.778 \pm 0.694$	Rutherford	1967	[67]
95.0	0.480 ± 0.030	$+0.389 \pm 0.087$	Harvard U.	1953	[59]
95.7	0.587 ± 0.029	$+0.137 \pm 0.056$	Harwell	1967	[40]
135.0	0.652 ± 0.154	$+0.023 \pm 0.241$	Harwell	1965	[68]
143.9	0.601 ± 0.057	$+0.109 \pm 0.105$	Harwell	1967	[40]
647.0	0.600 ± 0.080	$+0.111 \pm 0.148$	LAMPF	1976	[69]
800.0	0.660 ± 0.080	$+0.010 \pm 0.122$	LAMPF	1976	[69]

Table 5. **The** $R_{\mathrm{QE}}(\pi)$ **and** $R_{\mathrm{QE}}^{\mathrm{ID}}(\pi)$ **data measured using the reaction (1.8c).** **The uncertainties are total errors**

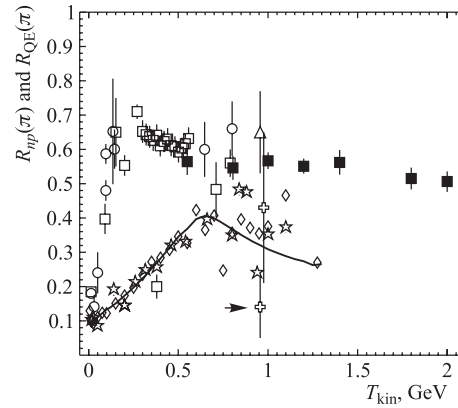| T_{kin}, MeV	$R_{\mathrm{QE}}(\pi)$	$R_{\mathrm{QE}}^{\mathrm{ID}}(\pi)$	Laboratory	Year	Ref.
977.0	0.140 ± 0.090	$+3.762 \pm 1.095$	JINR VBLHE	1975	[34]
	0.430 ± 0.220	$+0.550 \pm 1.008$			
977.0	0.650 ± 0.120	$+0.026 \pm 0.190$	JINR VBLHE	2002	[37]

Fig. 3. The energy dependence of the observable $R_{np}(\pi)$ and experimental points of $R_{QE}(\pi)$. The solid curve was calculated from ED GW/VPI PSA [53] (solution SP04). Diamonds — R_{np} from GW/VPI PSA [53] SES (sol. SP05), empty stars — R_{np} from SG PSA [54] (sol. 2007). Empty squares are the world data obtained using the reaction (1.8a), black squares are the recent Dubna points measured by the same reaction, open circles were obtained using the reaction (1.8b). Remaining points were measured using the reaction (1.8c) and the bubble chamber. Big empty crosses are the results from [34] and the arrow shows the point which is to be removed. The point from [37], corrected in 2006, is shown as the empty triangle
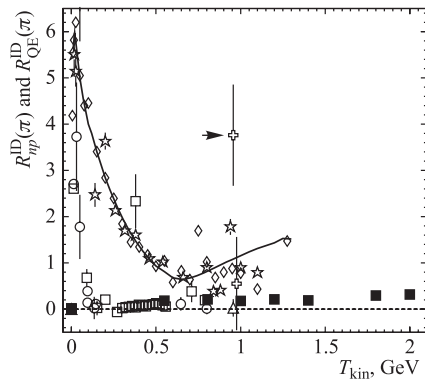
Fig. 4. The energy dependence of the observable $R_{np}^{ID}(\pi)$ and the experimental points of $R_{QE}^{ID}(\pi)$. The symbols are the same as in Fig. 3
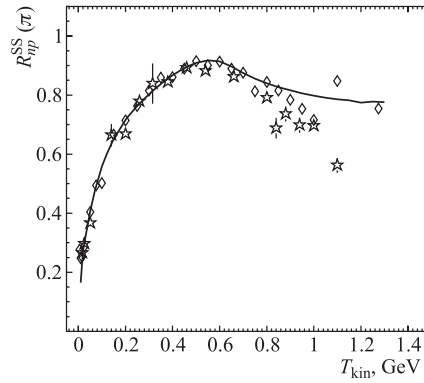
Fig. 5. The energy dependence of the observable $R_{np}^{SS}(\pi)$. The solid curve is calculated from ED GW/VPI PSA [53] (solution SP04). Diamonds — from GW/VPI PSA [53] SES (sol. SP05), empty stars — from SG PSA [54] (sol. 2007)

$R_{\mathrm{QE}}(\pi)$ data from Tables 3–5 are plotted in Fig. 3 and $R_{\mathrm{QE}}^{\mathrm{ID}}(\pi)$ values are shown in Fig. 4. In both figures, Figs. 3 and 4, the 22 data points from [41,52,57, 58,60–65] are shown as empty squares. The recent Dubna points [15] are plotted as full squares. The point of the same authors, measured at 0.55 GeV in March 2007, is still unpublished. The nine points from [40, 59, 66–69] (Table 4) are plotted as open circles. Two points from [34] (only one of them is independent) are plotted as big crosses, the point from [37], corrected by V. V. Glagolev (see below), is shown as an empty triangle (see Table 5).

The 33 independent data points published before 2003 cover the energy interval below 1 GeV. The statement in [37] that «such experimental data do not exist yet» could be hardly understood.

The experimental points measured at the JINR VBLHE Nuclotron are still preliminary [15]. They were obtained using the DELTA–SIGMA experimental equipment. Only these points show the $R_{\mathrm{QE}}(\pi)$ (and $R_{\mathrm{QE}}^{\mathrm{ID}}(\pi)$) energy dependence above 1 GeV, which could not be predicted from the previous data. It is worthwhile completing experiments with measurements in small energy steps, in order to recognize possible anomalies or structures. It is also desirable to extend the investigated interval up to the highest neutron energy at the Nuclotron (around 3.7 GeV). At present such a measurement is possible at this accelerator only.

The energy dependences of $R_{\mathrm{QE}}(\pi)$ and $R_{\mathrm{QE}}^{\mathrm{ID}}(\pi)$ data from [41, 52, 58, 62, 63,65,69] were shown in 1988 in [52]. The first comparison of the QE data and the PSA np predictions was shown in 1991 in [35], but without any conclusion. The energy interval was taken from 100 to 600 MeV, and the data from [52] were plotted together with the two ED PSA predictions from [70, 71]. Both fits in the restrained interval agree well with the fit from [53], solution SP04, shown in Fig. 4.

The quasi-elastic data plotted in Figs. 3 and 4 show smooth energy dependence for any reaction (1.8) used. The np PSA predictions and the quasi-elastic data differ considerably. Some papers referred to in Tables 3–5 need comments and the two existing anomalies are discussed below.

At small energies the data of Wong et al. [66] measured at LRL, Livermore, could not be read from the original paper. Fortunately, these data were shown in [64], together with the results obtained at the Kurchatov Atomic Energy Institute, Moscow. Experimental errors are not given. In other experiments at low energies (see, e.g., [72]), authors obtained enough of data, but published other interesting results only (e.g., NN scattering lengths).

The experiment described in [68] was performed in Harwell (UK) using a high-pressure Wilson cloud chamber, triggered by counters. The results from 1048 photographs of pd collisions were included in the final data analysis. In this paper the authors from the University College (London) in 1965 for the first time stated, «It is clear that the present results are consistently higher than theory».

The authors of [58] give the value $R_{\mathrm{QE}}(\pi) > 2/3$. The difference is of about two statistical errors. Consequently, the $R_{\mathrm{QE}}^{\mathrm{ID}}(\pi)$ value is slightly negative. Considering this point as a statistical fluctuation, one could state that all other values are smaller than 2/3.

Compared with other data, the $R_{\mathrm{QE}}(\pi)$ value from [60, 61] is considerably smaller. To understand this fact is not easy and the authors gave no comment. The reaction (1.8a) was investigated using the neutron beam and a scintillation counter array. Angles of outgoing protons could be well determined. At 380 MeV, not far from the pion-production threshold, the inelastic background is small and a magnetic analysis of outgoing protons can be omitted. The authors measured the angular distribution for this reaction as well as for the elastic np scattering. They observed an increase of $(d\sigma/d\Omega)_{np}$ in the backward hemisphere with increasing slope towards the backward proton direction.

The angular dependence of the nd differential cross section in a large angular region was found to be parallel to that for the np angular dependence. Obviously $(d\sigma/d\Omega)_{nd} < (d\sigma/d\Omega)_{np}$ due to the shadow effect of the nucleons in the deuteron. At an angle $\theta_{\mathrm{CM}} < \pi$, the values of $(d\sigma/d\Omega)_{nd}$ reached a maximum and then decreased towards the backward direction of outgoing protons. The spectator particles were neglected. The ratio $R_{\mathrm{QE}}(\theta_{\mathrm{lab}})$ at different outgoing proton angles was plotted. It reaches a sharp minimum in the backward direction, increases considerably with the increasing outgoing proton angle and becomes constant over a measured angular interval. The value of the constant is related to the Glauber corrections.

It should be noted that the sharp minimum in the backward direction was not observed in other experiments. Several authors measured $(d\sigma/d\Omega)_{nd}(\theta)$ accurately. At the 14 energies from 300 to 557 MeV measured in [52] the minimum is very weak, if any. At 152 MeV in [65] the angular dependence similar to that in [60, 61] can be seen, but the backward minimum is considerably weaker. A weak minimum also exists in the data at 977 MeV [34]. In [41] at 794 MeV no minimum was observed.

The experimental point from [60, 61] was included in the compilations [73, 74]. This controversial point is mentioned in [41, 65] without any comment. The point is discussed in [69] where is written, «This low value may indicate an anomaly behaviour in the spin-flip probability at this energy». The authors of [69] cannot know the accurate data from [52], which cover this energy region.

Only in [34, 37] the authors investigated reaction (1.8c), using the deuteron beam and the liquid hydrogen bubble chamber. The methods used in [34] and [37] to determine the desirable ratio were different.

In [34] the authors measured the $d\sigma/dt$ distribution for dp charge-exchange events. They considered the interaction as a charge-exchange reaction when the neutron momentum was higher than that of each of the protons in the deuteron rest system. The authors stated that this definition provides good separation of the

charge exchange and the charge retention channel events for the values of the four-momentum transfer from the proton to the neutron of less than ~ 0.6 $(\mathrm{GeV}/c)^2$.

The Glauber model predictions (neglecting the spin) were calculated with the formula given by Glauber and Franco [75]. The necessary t-dependence of the elastic scattering charge-exchange amplitude was approximated by a sum of two exponential functions, and the free parameters were obtained from the fit to np elastic scattering differential cross sections. Two sets of np data were used: data given by Shepard et al. [76] and by Bizard et al. (final data in [77] on the graph, tables in [74]). The influence of the deuteron effects was then obtained from the comparison of dp and np results. The authors of [34] stressed that their normalization is absolute.

The differential cross section for the reaction (1.8c) was computed using the form factor obtained by Alberi et al. [78] on the basis of the Bressel–Kerman deuteron wave function.

In [34] two values of the observable $R_{\mathrm{QE}}^{\mathrm{SI}}(\pi)$ (see Eq. (1.6)) were obtained, depending on the $(d\sigma/d\Omega)_{np}$ data used for the exponential fit. The corresponding $R_{\mathrm{QE}}(\pi)$ and $R_{\mathrm{QE}}^{\mathrm{ID}}(\pi)$ values are given in Table 5, where the upper result was calculated using the np data from [76] and the lower result using [77]. One observes that the upper value in Table 5 and the points denoted by arrows in Figs. 3 and 4 considerably differ with respect to other existing data. This difference could be easily explained.

In [76] are listed apparently very attractive $(d\sigma/d\Omega)_{np}$ results. They were measured at 16 energies and in large angular intervals at PPA (Pennsylvania Proton Accelerator), but strongly disagree with all other existing np data. Not only the absolute values, but also the shapes of angular distributions are different and the data cannot be renormalized. This occurs at all measured energies, starting at 182 MeV.

Physicists working in the field have long been well aware that these data are to be omitted. The [76] data were removed from all PSA databases (e.g., from SG PSA in 1978). For a demonstration, the data from [76] at 1.028 GeV are plotted together with the data from [77] at 1.029 GeV in Fig. 6. The fit of ED GW/VPI PSA (solution SP05) is also shown.
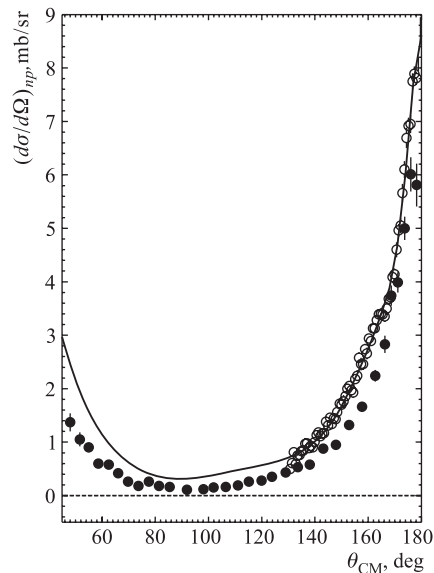

Fig. 6. The CM angular dependence of $(d\sigma/d\Omega)_{np}$ at 1.028 GeV. Black dots are from [76], open circles from [77] and the solid line is from [53] (solution SP05)

Only the second result from [34] in Table 5 is to be taken into account. It is compatible with other data. The authors of [34] in 1975 could hardly recognize a quality of the data from [76].

The paper [37] investigated the reaction (1.8c) at the same energy as in [34], but with increased statistics. To determine the angular dependence of the quasi-elastic dp differential cross section in the charge-exchange region, the kinematic variable in [37] was the opening angle ω of the cone around the incident deuteron direction. The angles of both outgoing final protons are to be inside this cone. The measured differential cross section $(d\sigma/dt)_{dp}$ as a function of ω is plotted in the original paper. It was shown that the cross section increases with increasing ω and becomes rapidly constant.

The angle of any of the two protons was estimated using the experimental and theoretical maxima of the Fermi momentum distribution of the nucleons in the deuteron (50 MeV/c) and the longitudinal momentum of incident deuteron per nucleon (1.67 GeV/c). The authors considered that this requirement is a sufficient condition for the charge-exchange scattering, since the opening angle of the cone $\omega = 3°$ covers practically the entire «spectator peak». Based on this estimation, Glagolev et al. observe that at this opening angle the measured $(d\sigma/d\Omega)_{dp}$ represents 94% of $(2/3)\,(d\sigma/d\Omega)_{np}(\pi)$.

Here is an additional difficulty related to the measurement of the reaction (1.8c). The number of events decreases with decreasing ω and the measured differential cross section ratios need corrections. The authors of [37] in private communications advertized that these corrections were not introduced in their results and even were not known. From this it followed that one cannot calculate the ratio $R_{\mathrm{QE}}^{\mathrm{ID}}(\pi)$ at different values of ω from the graph given in [37].

The value of $(d\sigma/d\Omega)_{np}(\pi) = 5.81$ mb/sr was taken again from [76]. With respect to [34], it is hardly believable that in 2002 the result from [76] and no other one was used. The authors surprisingly gave the result $R_{\mathrm{QE}}(\pi) = 0.630 \pm 0.101$ ($R_{\mathrm{QE}}^{\mathrm{ID}}(\pi) = 0.058 \pm 0.170$), which is in full agreement with other existing measurements. Based on this fact, the authors declared that at 1.67 GeV/c «the $np \to pn$ amplitude turned out to be entirely spin-dependent».

This statement, often repeated throughout [37] (abstract, text, conclusion), is obviously wrong and misleading. As was explained above, the spin-dependent and spin-independent parts of the $np \to np$ differential cross section at $\theta_{\mathrm{CM}} = \pi$ are related to the observables $R_{np}(\pi)$ or $R_{np}^{\mathrm{ID}}(\pi)$ given in Table 2. On the other hand, the authors show that the theory and the experiment disagree independently of their opinion.

In January 2006 Glagolev et al. recalculated their result published in [37]. They introduced corrections for the differential dp cross sections at small angles ω, taking into account cuts of events as a function of ω. The authors used the normalization related to the np differential cross section from [77]. This new result is listed in Table 5.

In [37] some other statements cannot be taken into account seriously. As example, the statement that «all dedicated charge-exchange experiments on a deuteron so far have been carried out with proton beams» is in contradiction with Table 3. Another statement concerning the Brookhaven np data of Friedes et al. [79] is to be considered as a mistake.

Let me note that a considerable amount of $(d\sigma/d\Omega)_{np}$ data in the charge-exchange angular region exists, up to the highest energies (see, e.g., [80] at 270 GeV/c). Unfortunately, many original papers contain graphs only, but a majority of the numerical tables was obtained from authors and the data were listed. For examples, see [73, 74, 81] or the PSA database of Arndt et al. [53]. The energy dependence of $(d\sigma/dt)_{np}$ in the backward direction was fitted in [82].

9. CONCLUSIONS

The present paper recalls the expressions for the np elastic backward scattering differential cross section $(d\sigma/d\Omega)_{np}$, its spin-independent and spin-dependent parts as functions of scattering amplitudes. Five amplitude representations are compared and the corresponding formulae are checked. Some expressions for the charge-exchange amplitudes are also shown.

The predictions of the spin-independent and spin-dependent parts of the np cross sections were calculated using the three PSA. Energy dependences of measured quasi-elastic and calculated elastic results are presented in tables and shown in figures. They differ considerably over the PSA energy interval and lead to the conclusion that the quasi-elastic observables under discussion cannot contribute to our knowledge of the np elastic scattering amplitudes in the backward direction. An explanation of the observed difference is highly desirable and needs a serious theoretical approach.

It can be seen that the measurement of the reaction (1.8a) has several considerable advantages over the reaction (1.8b) and even crucial advantages over the measurement of the reaction (1.8c). The number of measured data points for each of these reactions confirms this statement.

The measurements of $R_{QE}(\pi)$ at the Nuclotron in the region of $T_{kin}(n)$ from 1 to 2 GeV can be considered as an important achievement in this field. From the preliminary Dubna data it is possible to estimate, for the first time, the behaviour of this observable over the high energy region.

Eugene Plekhanov, Eugene Strokovsky and Imrich Zborovský for their kind help concerning the present critical review.

Note added in proof.   The present article contains the determination of the spin dependent and independent parts of the np differential cross sections for incident neutrons scattered in the backward direction only. A complete description of these reactions was published in: *Lehar F., Wilkin C. //* Eur. Phys. J. A. 2008. V. 37. P. 143, and following details will be published in «Part. Nucl., Lett.», 2010. V. 7, No. 4.

REFERENCES

1. *Chew G. F. //* Phys. Rev. 1950. V. 80. P. 196.

2. *Chew G. F. //* Phys. Rev. 1951. V. 84. P. 710.

3. *Pomeranchuk I. //* Dokl. Akad. Nauk SSSR. 1951. V. LXXVII. P. 249.

4. *Watson K. M. //* Phys. Rev. 1952. V. 88. P. 1163.

5. *Shmushkevich I. M.* Thesis. Leningrad Phys.-Techn. Inst., 1953.

6. *Migdal A. B. //* ZhETF. 1955. V. 28. P. 3; Sov. Phys. JETP. 1955. V. 1. P. 2.

7. *Lapidus L. I. //* ZhETF. 1957. V. 32. P. 1437; Sov. Phys. JETP. 1957. V. 5. P. 1170.

8. *Dean N. W. //* Phys. Rev. D. 1972. V. 5. P. 1661.

9. *Dean N. W. //* Ibid. P. 2832.

10. *Bugg D., Wilkin C. //* Nucl. Phys. A. 1987. V. 167. P. 575.

11. *Phillips R. J. N. //* Nucl. Phys. 1964. V. 53. P. 650.

12. *Sharov V. I. et al. //* Eur. Phys. J. 2004. V. 37. P. 79.

13. *Sharov V. I. et al. //* Yad. Fiz. 2005. V. 68. P. 1858; Phys. At. Nucl. 2005. V. 68. P. 1796.

14. *Lehar F. //* Part. Nucl. 2005. V. 36. P. 955.

15. *Sharovet V. I. et al. //* Czech. J. Phys. 2006. V. 56. P. F117.

16. *Ladygina N. B., Shebeko A. V. //* Eur. Phys. J. A. 2004. V. 22. P. 29.

17. *Ladygina N. B. //* Yad. Fiz. 2008. V. 71, No. 12. P. 2073.

18. *Ellengaard C. et al. //* Phys. Rev. Lett. 1987. V. 59. P. 974.

19. *Ellengaard C. et al. //* Phys. Lett. B. 1989. V. 231. P. 365.

20. *Sams T. et al. //* Phys. Rev. 1995. V. 51. P. 1945.

21. *Kox S. et al. //* Nucl. Phys. A. 1993. V. 556. P. 621.

22. *Bugg D. V., Wilkin C. //* Phys. Lett. B. 1985. V. 152. P. 37.

23. *Wilkin C., Bugg D. V. //* Ibid. V. 154. P. 243.

24. *Komarov V. et al. //* Phys. Lett. B. 2003. V. 553. P. 179.

25. *Chiladze D. et al.* // Phys. Lett. B. 2006. V. 637. P. 170.

26. *Carbonell J., Barbaro M. B., Wilkin C.* // Nucl. Phys. A. 1991. V. 529. P. 653.

27. *Heidenbauer J., Uzikov Yu. N.* // Phys. Lett. B. 2003. V. 562. P. 227.

28. *Uzikov Yu. N., Heidenbauer J., Wilkin C.* // Phys. Rev. C. 2007. V. 75. P. 014008.

29. *Yaschenko S. et al.* // Phys. Rev. Lett. 2005. V. 94. P. 072304.

30. *Bystrický J., Lehar F., Winternitz P.* // J. Phys. (Paris). 1978. V. 39. P. 1.

31. *La France P., Winternitz P.* // J. Phys. (Paris). 1980. V. 41. P. 1391.

32. *Lechanoine-Leluc C., Lehar F.* // Rev. Mod. Phys. 1993. V. 65. P. 47.

33. *Jacob M., Wick G. C.* // Ann. Phys. (N. Y.). 1959. V. 7. P. 404.

34. *Aladashvili B. S. et al.* // Nucl. Phys. B. 1975. V. 86. P. 461.

35. *Binz R.* Untersuchung der spinabhängigen Neutron–Proton Wechselwirkung im Energiebereich von 150 bis 1100 MeV. Thesis. Albert-Ludwigs-Universität, Freiburg im Breisgau, 1991 (unpublished).

36. *Goldberger M., Watson K.* Collision Theory. N. Y.: Wiley, 1966.

37. *Glagolev V. V. et al.* // Eur. Phys. J. A. 2002. V. 15. P. 471.

38. *Stapp H. P.* The Theory and Interpretation of Polarization Phenomena in Nuclear Scattering. Thesis. UCRL-3098. Berkeley, 1955.

39. *Stapp H. P., Ypsilantis T. J., Metropolis N.* // Phys. Rev. 1957. V. 105. P. 302.

40. *Langsford A. et al.* // Nucl. Phys. 1967. V. 99. P. 246.

41. *Bonner B. E. et al.* // Phys. Rev. C. 1978. V. 17. P. 664.

42. *Wolfenstein L., Ashkin J.* // Phys. Rev. 1952. V. 85. P. 947.

43. *Wolfenstein L.* // Phys. Rev. 1954. V. 96. P. 1054.

44. *Wolfenstein L.* // Phys. Rev. 1956. V. 101. P. 427.

45. *Wolfenstein L.* // Ann. Rev. Nucl. Sci. 1956. V. 6. P. 43.

46. *Bilenky S. M., Ryndin R. M.* // Phys. Lett. 1963. V. 6. P. 217.

47. *Phillips R. J. N.* // Nucl. Phys. 1963. V. 43. P. 413.

48. *Grein W., Kroll P.* // Nucl. Phys. 1982. V. 277. P. 505.

49. *Kroll P.* Phenomenological Analyses of Nucleon–Nucleon Scattering. Physics Data No. 22–1 / Eds.: H. Behrens und G. Ebel. Karlsruhe: Fachinformationszentrum, 1981.

50. *Ball J. et al.* // Eur. Phys. 1998. V. 5. P. 57.

51. *Halzen F., Thomas G. H.* // Phys. Rev. 1974. V. 10. P. 344.

52. *Pagels B.* Untersuchung der quasielastischen Ladungsaustauschreaktion $nd \rightarrow pnn$ im Neutronenergiebereich von 290 bis 570 MeV. Diplomarbeit. Fakultät für Physik der Universität Freiburg im Breisgau, 1988 (unpublished).

53. *Arndt R. A., Strakovsky I. I., Workman R. L.* // Phys. Rev. C. 2000. V. 62. P. 034005.

54. *Bystrický J., Lechanoine-LeLuc C., Lehar F.* // Eur. Phys. C. 1998. V. 4. P. 607.

55. *Adams D. et al. //* Acta Polytechnica (Prague). 1996. V. 36. P. 11.

56. *de Lesquen A. et al. //* Eur. Phys. J. C. 1999. V. 11. P. 69.

57. *Powell W. M.* Preprint UCRL 1191. Berkeley, 1951.

58. *Cladis J. R., Hadley J., Hess W. N. //* Phys. Rev. 1952. V. 86. P. 110.

59. *Hofmann J. A., Strauch K. //* Phys. Rev. 1953. V. 90. P. 559.

60. *Dzhelepov V. P. et al. //* Izv. Akad. Nauk. 1955. V. 19. P. 573.

61. *Dzhelepov V. P. et al. //* Nuovo Cim. Suppl. 1956. V. 3. P. 61.

62. *Larsen R. R. //* Nuovo Cim. 1960. V. 18. P. 1039.

63. *Dzhelepov V. P.* Recent Investigations on Nucleon–Nucleon Scattering at the Dubna Synchrocyclotron // Proc. of the 1962 Intern. Conf. on High-Energy Physics, CERN, Geneva, July 4–11, 1962 / Ed. by J. Prentki. P. 19.

64. *Voitovetskii V. K., Korsunskii I. L., Pazhin Yu. F. //* Nucl. Phys. 1965. V. 69. P. 531.

65. *Measday D. F. //* Phys. Lett. 1966. V. 21. P. 66.

66. *Wong C. et al. //* Phys. Rev. 1959. V. 116. P. 164.

67. *Batty C. J., Gilmore R. S., Stafford G. H. //* Phys. Lett. 1965. V. 16. P. 137.

68. *Esten M. J. et al. //* Rev. Mod. Phys. 1965. V. 37. P. 533.

69. *Bjork C. W. et al. //* Phys. Lett. B. 1976. V. 63. P. 31.

70. *Arndt R. A., Hyslop J. S., III, Roper L. D.* Interactive Program SAID // Phys. Rev. 1987. V. 35. P. 199.

71. *Bystrický J., Lechanoine-Leluc C., Lehar F. //* J. Phys. (Paris). 1987. V. 48. P. 199.

72. *Cerineo M. et al. //* Phys. Rev. B. 1964. V. 133. P. 948.

73. *Bystrický J., Lehar F., Janout Z.* Elastic Nucleon–Nucleon Scattering Data 270–3000 MeV. Note CEA-N-1547(E). Saclay, 1972.

74. *Bystrický J., Lehar F.* Nucleon–Nucleon Scattering Data / Eds. H. Behrens und G. Ebel. Karlsruhe: Fachinformationszentrum, 1978–1981. Edition Nr. 11-1. 1978; Edition Nr. 11-2. 1981; Nr. 11-3. 1981.

75. *Glauber J. R., Franco V. //* Phys. Rev. 1967. V. 156. P. 1685.

76. *Shepard P. F. et al. //* Phys. Rev. D. 1974. V. 10. P. 2735.

77. *Bizard G. et al. //* Nucl. Phys. B. 1975. V. 85. P. 14.

78. *Alberi G., Bertocchi L., Bialkovski G. //* Nucl. Phys. B. 1970. V. 17. P. 621.

79. *Friedes J. L. et al. //* Phys. Rev. Lett. 1965. V. 15. P. 38.

80. *Barton H. R., Jr., et al. //* Phys. Rev. Lett. 1976. V. 37. P. 1656.

81. *Bystrický J. et al.* Elastic and Charge-Exchange Scattering of Elementary Particles a: Nucleon–Nucleon and Kaon–Nucleon Scattering. Landolt-Börnstein, New Series. V. 9 / Ed. H. Schopper; Editor in Chief: K. H. Hellwege. Group I: Nucl. Part. Phys. Berlin; Heidelberg; N. Y.: Springer-Verlag, 1980.

82. *Strokovsky E. A. //* Part. Nucl., Lett. 2004. V. 1, No. 2(119). P. 5.